Electronic Supplementary Material (ESI) for ChemComm.

Use of modulators and light to control crystallization of a hydrogen bonded framework

Phonlakrit Muang-Non[†], Hamish D. Toop[‡], Christian J. Doonan[‡] and Nicholas G. White[†*]

[†]*Research School of Chemistry, The Australian National University, 137 Sullivan's Creek Road, Acton, 2600, ACT, Australia; Email: nicholas.white@anu.edu.au URL: www.nwhitegroup.com*

[‡]*Department of Chemistry and the Centre for Advanced Nanomaterials, The University of Adelaide, Adelaide, South Australia 5005, Australia.*

Synthesis of new compounds

General remarks

Tetraamidinium **1·Cl$_4$**, and the potassium salt of **DiA^{2-}** were prepared as previously described.[1] The new tetrabutylammonium (TBA) salts of stilbenedicarboxylate and naphthalenedisulfonate, *i.e.* **TBA$_2$·SB** and **TBA$_2$·NDS**, were prepared from commercially available 4,4′-stillbenedicarboxylic acid (**SB^{2H}**) and 1,5-naphthalenedisulfonic acid tetrahydrate (**NDS^{2H}·4H$_2$O**), respectively (Scheme S1). All other chemicals (including solvents) were bought from commercial suppliers and used as received. NMR spectra were collected on Bruker Avance 400 and are referenced to the residual solvent signal. Infrared spectra were recorded on a Perkin-Elmer Spectrum Two FT-IR Spectrometer fitted with an ATR Two Single Reflection Diamond. Electrospray ionisation mass spectrometry data were acquired on a Micromass Waters ZMD spectrometer. PXRD data were collected using a PANalytical diffractometer with Cu K$_\alpha$ radiation and a PIXcel detector. TGA data were recorded on a TA Instruments Q500 analyser under flowing nitrogen at a ramp speed of 5 °C/minute. SEM data were collected on an FEI QEMSCAN 650F microscope operating at 15 kV, with a 3 nA probe current and 15 mm working distance. Samples were dispersed on a glass slide, dried and then sputter-coated with 25 nm graphite before data collection. Crystal dimensions have not been altered to account for this graphite layer.

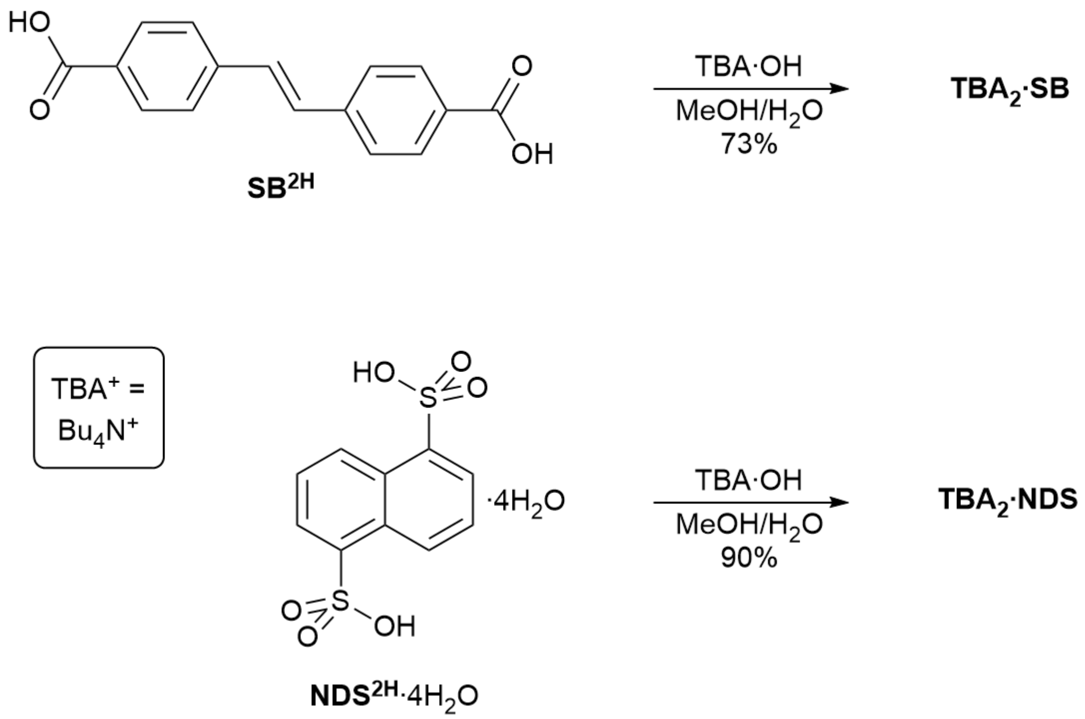

Scheme S1. Synthesis of **TBA$_2$·SB** and **TBA$_2$·NDS**.

Synthesis and characterisation of TBA$_2$·SB

4,4′-Stilbenedicarboxylic acid (55 mg, 0.21 mmol) was suspended in water (5 mL). Tetrabutylammonium hydroxide in methanol (1.0 M, 1.0 mL) was added to the reaction mixture and stirred for 10 minutes. The reaction mixture was dried *in vacuo*, giving a brown powder. Excess tetrabutylammonium hydroxide was removed by dissolving the crude material in hot acetone (5 mL) and precipitating using diethyl ether (20 mL). The resulting white powder was isolated by filtration, washed with diethyl ether (2 × 10 mL) and air-dried. Yield: 0.11 g (73%)

Characterisation Data: ^{1}H NMR (400 MHz, d$_6$-DMSO): 7.78 (d, *J* = 8.2 Hz, 4H), 7.43 (d, *J* = 8.2 Hz, 4H), 7.19 (s, 2H), 3.12–3.21 (m, 16H), 1.52–1.63 (m, 16H), 1.26–1.35 (m, 16H), 0.93 (t, *J* = 7.3 Hz) ppm. ^{13}C (101 MHz, d$_6$-DMSO): 167.8, 141.4, 136.6, 129.3, 128.1, 125.1, 57.5, 23.1, 19.2, 13.5 ppm. ESI-MS (neg.): 508.3, calc. for $[C_{32}H_{46}NO_4]^-$, *i.e.* [**TBA·SB**]$^-$ = 508.3 Da.

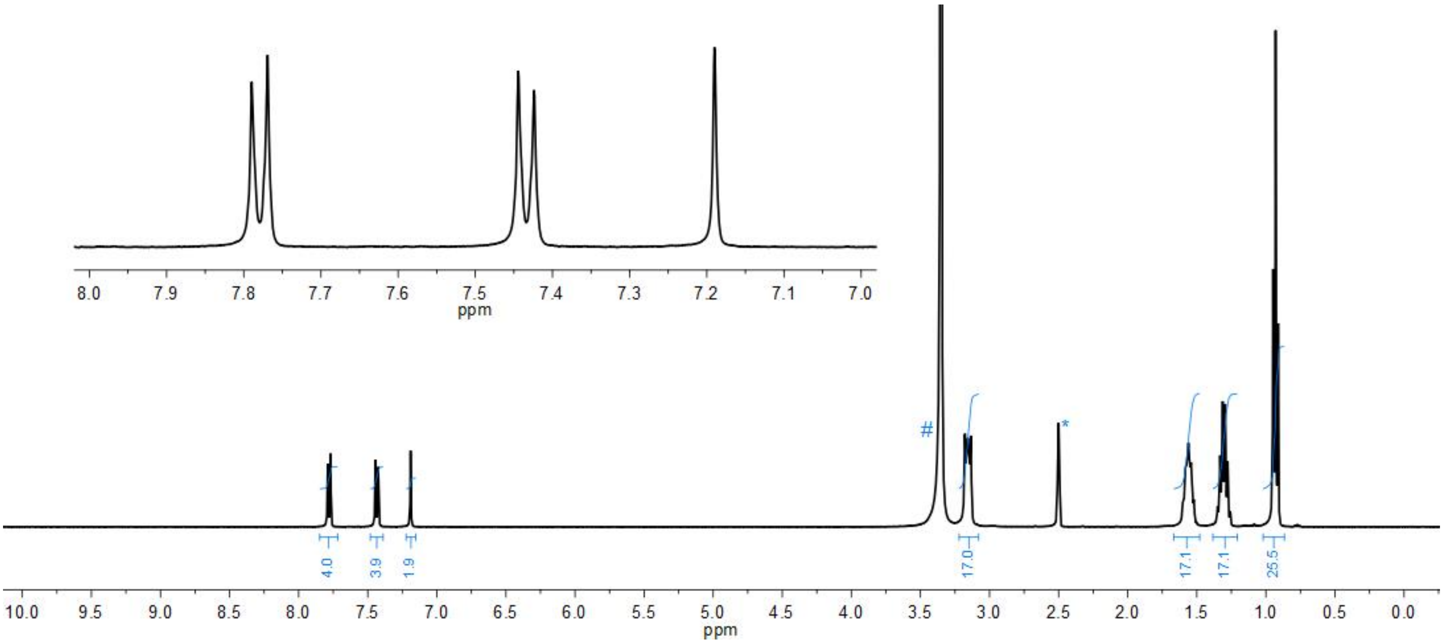

Figure S1. ^{1}H NMR spectrum of **TBA$_2$·SB**, peak labelled * results from incompletely deuterated NMR solvent, peak labelled # results from water (d$_6$-DMSO, 400 MHz, 298 K).

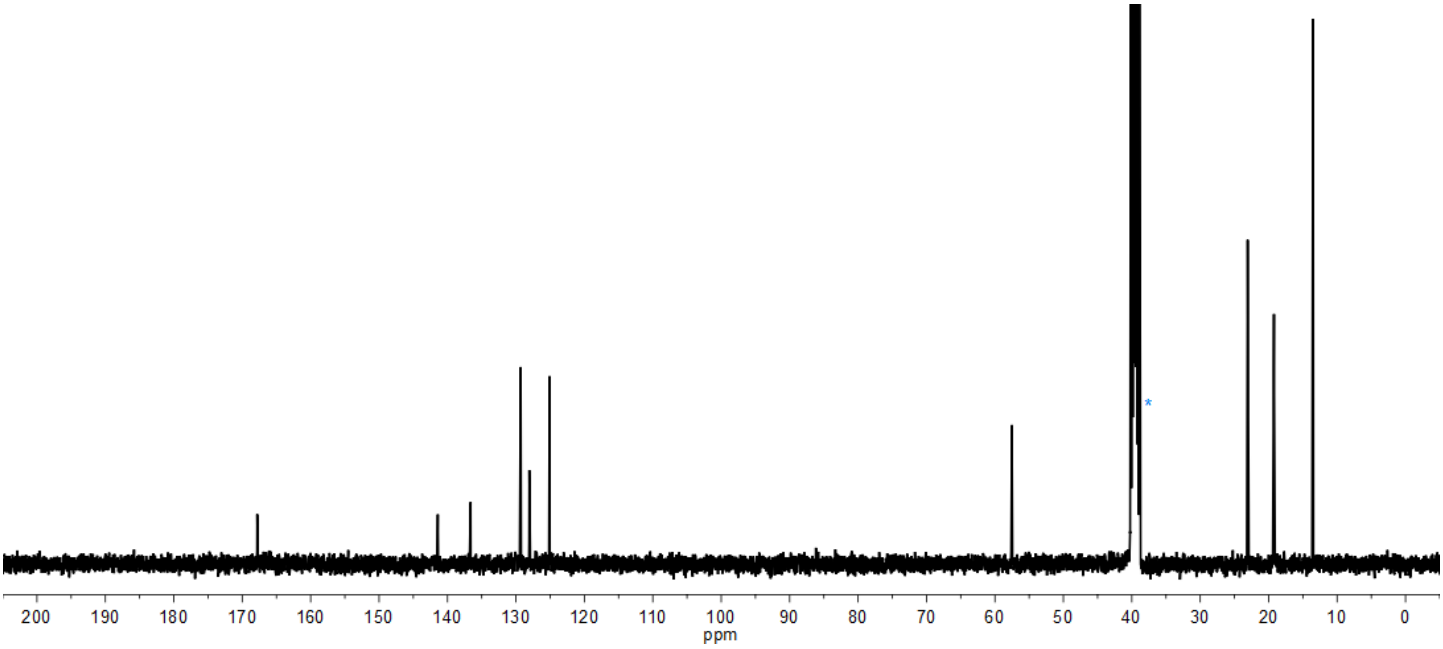

Figure S2. ^{13}C NMR spectrum of **TBA$_2$·SB**, peak labelled * results from incompletely deuterated NMR solvent (d$_6$-DMSO, 101 MHz, 298 K).

Synthesis and characterisation of TBA$_2$·NDS

1,5-Naphthalenedisulfonic acid tetrahydrate (50 mg, 0.14 mmol) was dissolved in water (5 mL). Tetrabutylammonium hydroxide in methanol (1.0 M, 0.28 mL) was added to the reaction mixture and stirred for 10 minutes. The reaction mixture was dried in *vacuo*, giving a brown powder. The product was recrystallized by dissolving in hot acetone (5 mL) and precipitating using diethyl ether (20 mL). The white powder was isolated by filtration, washed with diethyl ether (2 × 10 mL) and air-dried. Yield: 0.10 g (90%)

Characterisation Data: ^{1}H NMR (400 MHz, d$_6$-DMSO): 8.86 (d, J = 8.8 Hz, 2H), 7.92 (dd, J = 7.0, 1.0 Hz, 2H), 7.40 (dd, J = 8.8, 7.0 Hz), 3.12–3.21 (m, 16H), 1.51–1.61 (m, 16H), 1.26–1.35 (m, 16H), 0.93 (t, J = 7.3 Hz, 24H) ppm. ^{13}C NMR (101 MHz, d$_6$-DMSO): 144.0, 129.6, 129.0, 123.9, 123.8, 57.5, 23.1, 19.2, 13.5 ppm. ESI-MS (neg.): 528.3, calc. for $[C_{26}H_{42}NO_6S_2]^-$, *i.e.* [**TBA·NDS**]$^-$ = 528.3 Da.

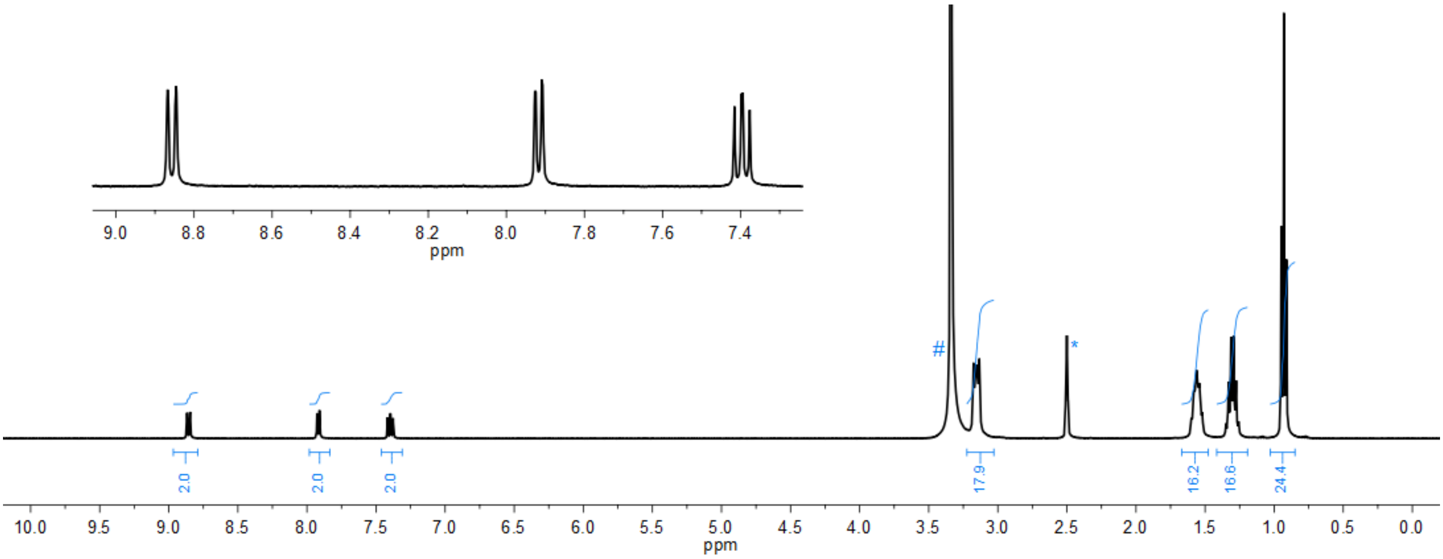

Figure S3. ^{1}H NMR spectrum of **TBA$_2$·NDS**, peak labelled * results from incompletely deuterated NMR solvent, peak labelled # results from water (d$_6$-DMSO, 400 MHz, 298 K).

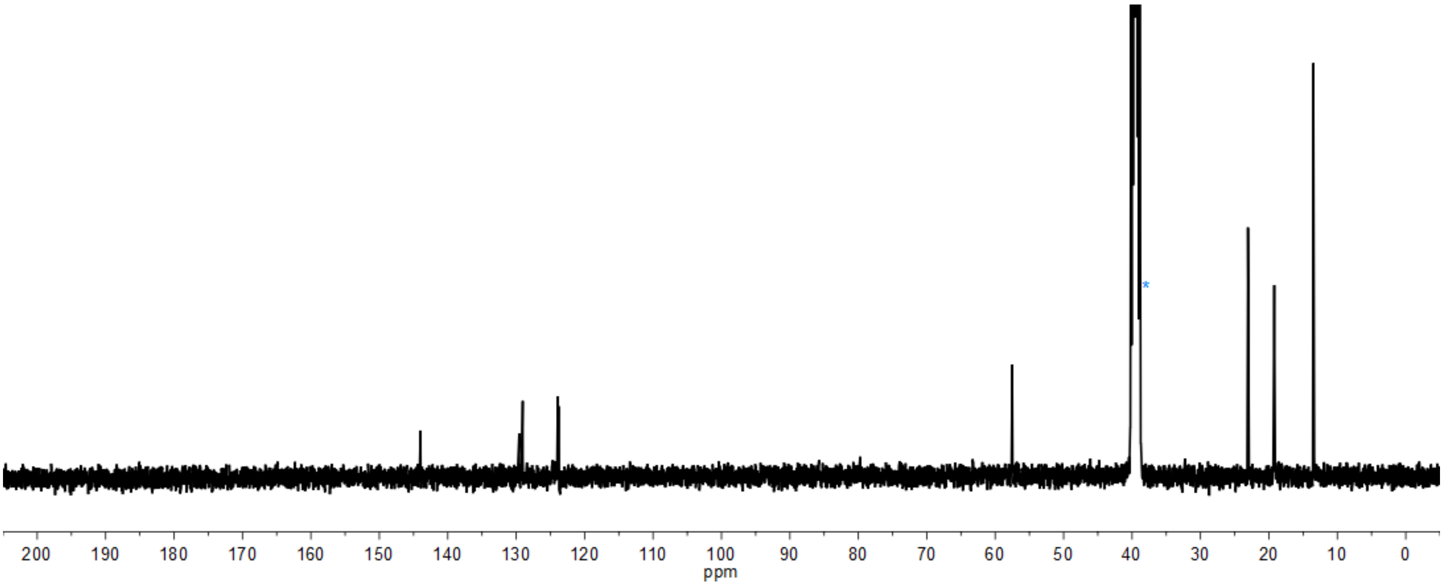

Figure S4. ^{13}C NMR spectrum of **TBA$_2$·NDS**, peak labelled * results from incompletely deuterated NMR solvent (d$_6$-DMSO, 101 MHz, 298 K).

Synthesis and characterisation of 1·DiA$_2$

K$_2$·DiA (6.92 mg, 20.0 µmol) was dissolved in 1:1 EtOH:H_2O (15 mL) and added to a solution of **1·Cl$_4$** (6.32 mg, 9.96 µmol) in 1:1 EtOH:H_2O (15 mL) and the orange solution left to stand at room temperature. Crystals began to form after approximately 5 minutes. After four days, the orange crystals were isolated by filtration, washed with water and air-dried. **Yield:** 0.011 g (9.0 µmol, 90%). *Yield calculated assuming 11 waters per repeating unit (as indicated by TGA)*.

Characterisation Data: ^{1}H NMR (d$_6$-DMSO containing a drop of conc. $HCl_{(aq)}$): 9.57 (br, s, 8H), 9.31 (br, s, 8H), 8.13 (d, *J* = 8.5 Hz, 8H), 7.98 (d, *J* = 8.5 Hz, 8H), 7.93 (d, *J* = 8.6 Hz, 8H), 7.52 (d, *J* = 8.6 Hz, 8H) ppm. ATR-IR (*inter alia*):, 1680, 1595, 1539 (C=N, C=O stretches) 1371 (C–N stretch) cm^{-1}. EA: C 59.3, H 5.4, N 14.6; calc. for $C_{57}H_{62}N_{12}O_{15}$ (*i.e.* **1·DiA$_2$**·7H_2O): C 59.3, H 5.4, N 14.6%.

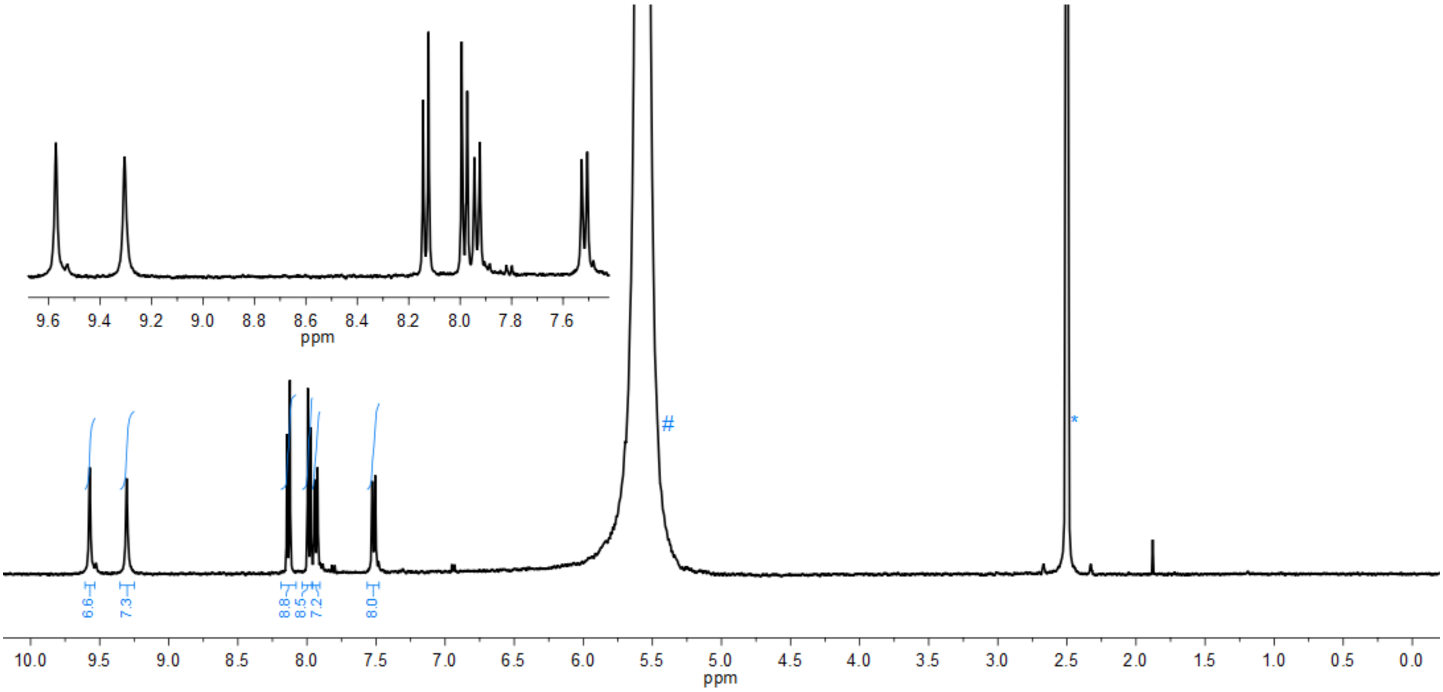

Figure S5. ^{1}H NMR spectrum of acid-digested **1·DiA$_2$**; peak labelled * results from incompletely deuterated NMR solvent, peak labelled # results from water (d$_6$-DMSO containing 1 drop $DCl_{(aq)}$, 400 MHz, 298 K).

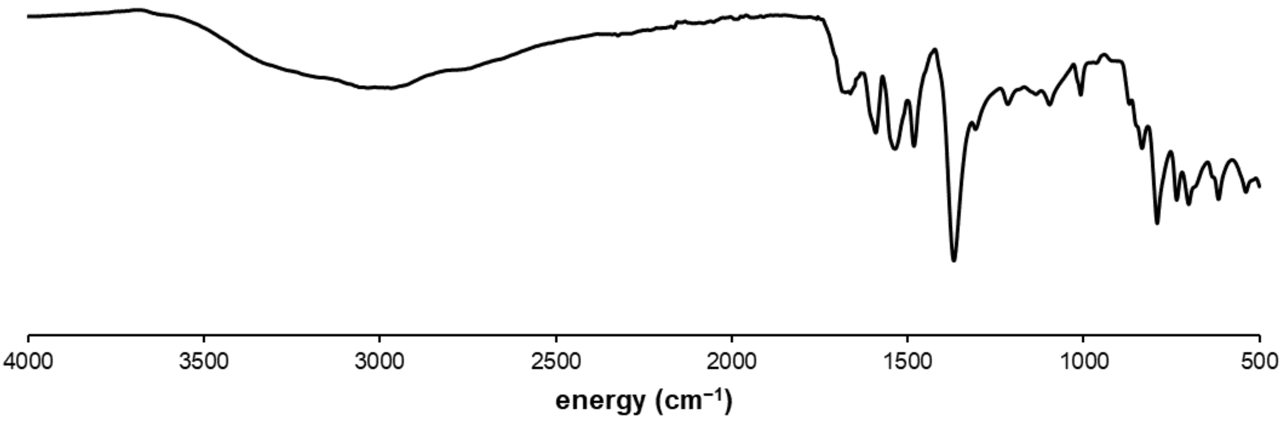

Figure S6. ATR-IR spectrum of **1·DiA$_2$**.

TGA data (Figure S7) are consistent with the framework containing 11 water molecules per repeating unit.

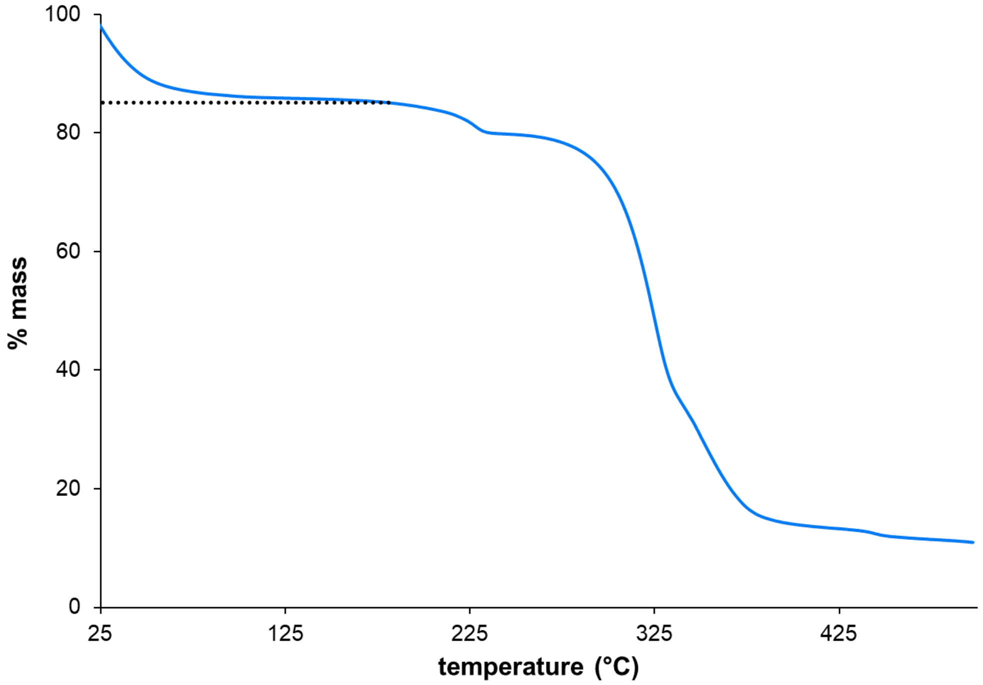

Figure S7. TGA trace of **1·DiA**$_2$. The dotted black line represents a mass loss corresponding to the loss of 11 waters per repeating unit (85.1%).

PXRD data (Figure S8) show that the dried material is amorphous. Adding a drop of water (at t = 0 mins) results in crystallinity being restored, but then eventually being lost, which we attribute to the water ordering the material and then slowly evaporating. The PXRD of the rehydrated material is consistent with that calculated from the SCXRD structure.

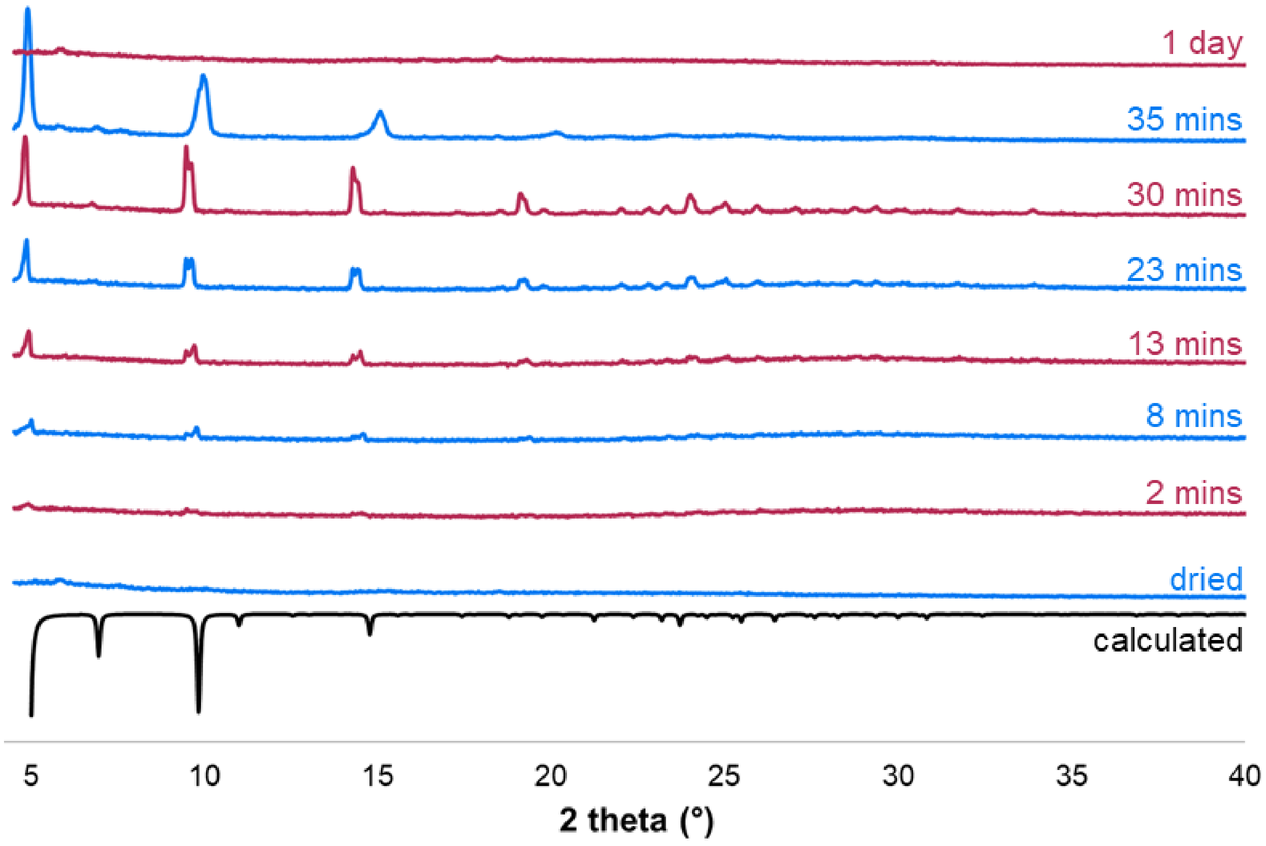

Figure S8. PXRD pattern of **1·DiA**$_2$, and at various times after the addition of water; “calculated” trace represents that predicted from the SCXRD structure.

Synthesis and characterisation of 1·SB$_2$

TBA$_2$·SB (15 mg, 20 µmol) was dissolved in 1:1 EtOH:H_2O (10 mL) and added to a solution of **1·Cl$_4$** (6.3 mg, 10 µmol) in 1:1 EtOH:H_2O (10 mL) and the colourless solution left to stand at room temperature. Crystals began to form after approximately 20 minutes. After four days, the colourless crystals were isolated by filtration, washed with water, and air-dried. **Yield:** 0.012 g (10 µmol, 100%). *Yield calculated assuming 9 waters per repeating unit (as indicated by TGA)*.

Characterisation Data: ^{1}H NMR (d$_6$-DMSO containing a drop of conc. $HCl_{(aq)}$): 9.58 (br. s, 8H), 9.33 (br. s, 8H), 7.91–7.96 (m, 16H), 7.74 (d, *J* = 8.4 Hz, 8H), 7.53 (d, *J* = 8.6 Hz, 8H), 7.47 (s, 4H) ppm. ATR-IR (*inter alia*): 1666, 1606, 1578, 1523, 1481 (C=N, C=O, C=C stretches), 1369 (C–N stretch) cm^{-1}. EA: C 59.2, H 5.5, N 9.8; calc. for $C_{61}H_{74}N_8O_{19}$ (*i.e.* **1·SB$_2$**·11H_2O): C 59.9, H 6.1, N 9.2%.

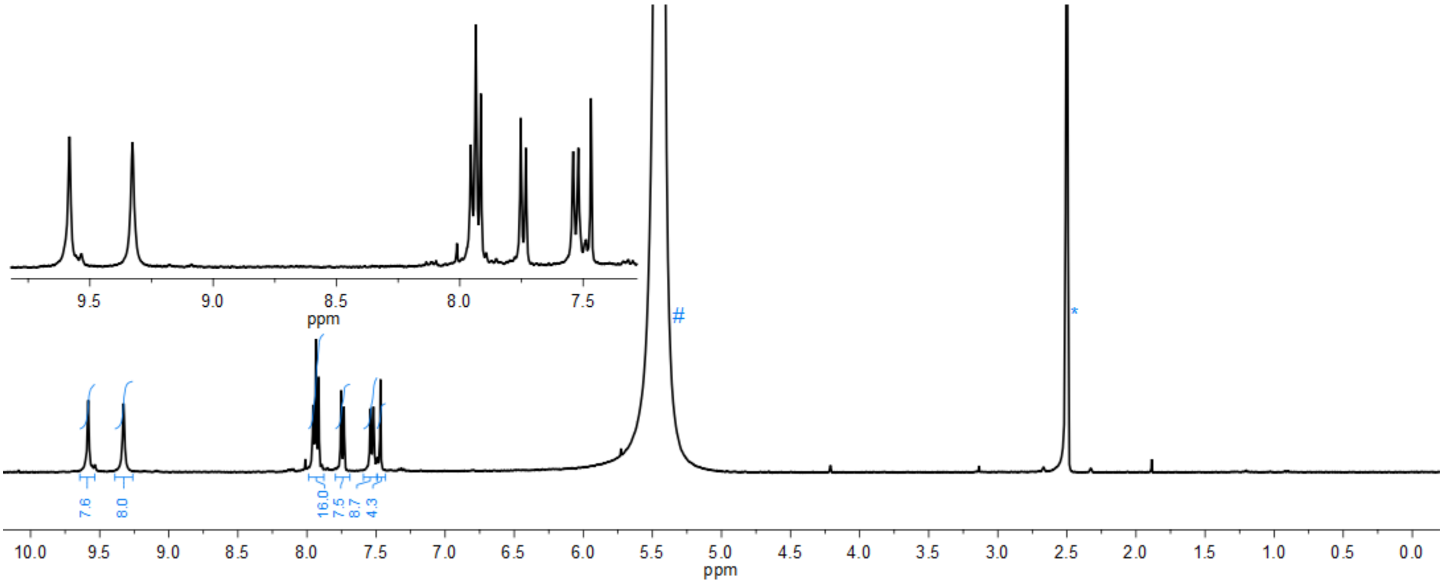

Figure S9. ^{1}H NMR spectrum of acid-digested **1·SB$_2$,** peak labelled * results from incompletely deuterated NMR solvent, peak labelled # results from water (d$_6$-DMSO containing a drop of $DCl_{(aq)}$, 400 MHz, 298 K).

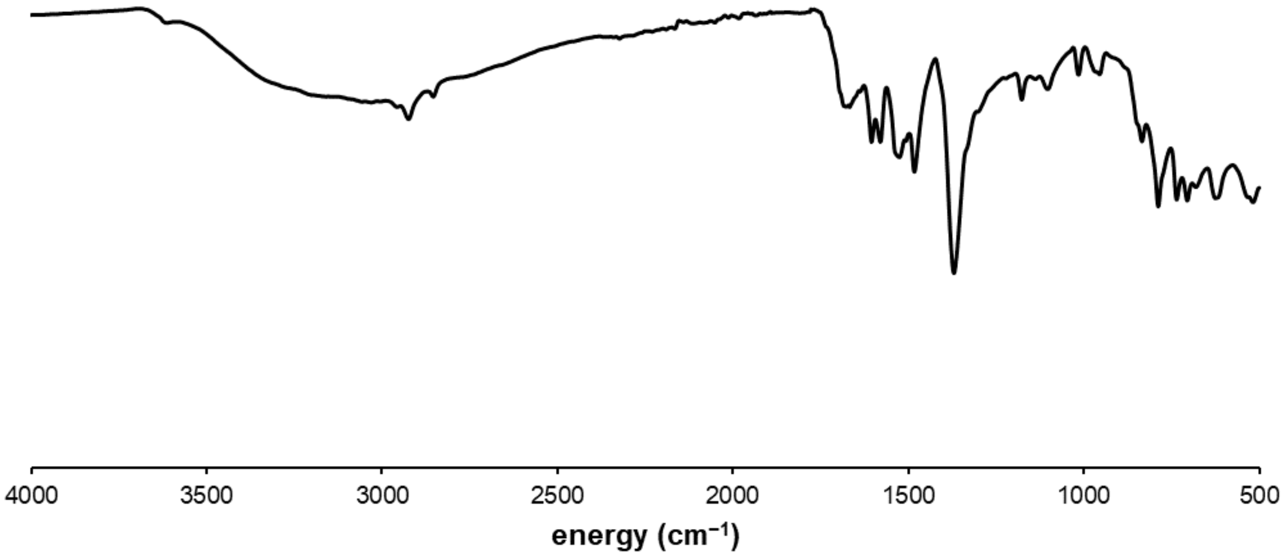

Figure S10. ATR-IR spectrum of **1·SB$_2$**.

TGA data (Figure S11) are consistent with the framework containing nine water molecules per repeating unit.

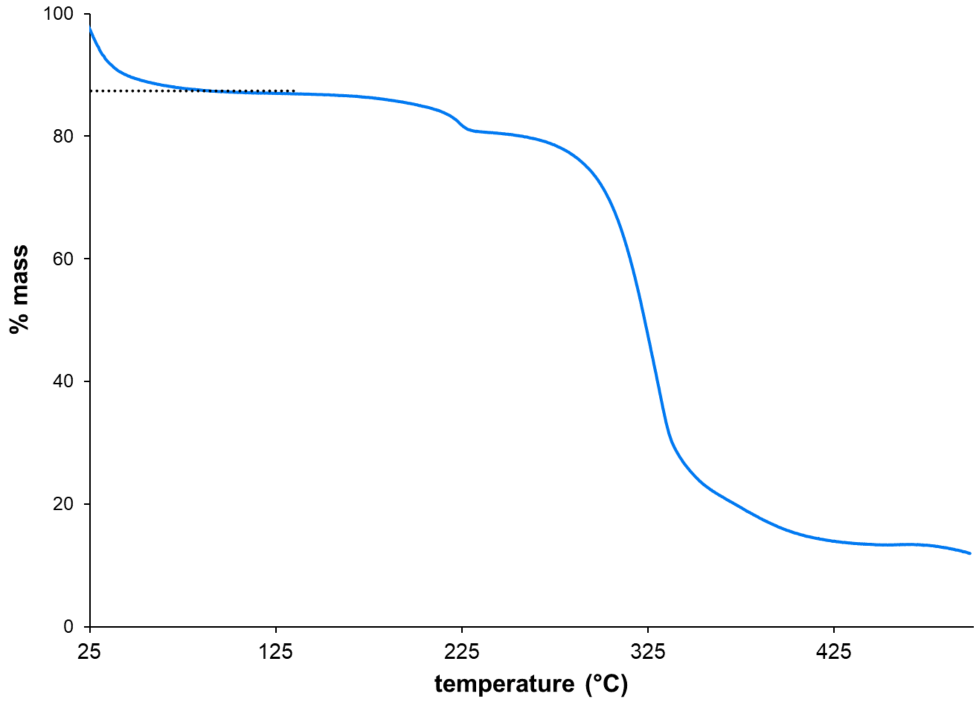

Figure S11. TGA trace of **1·SB**$_2$. The dotted black line represents a mass loss corresponding to the loss of nine waters per repeating unit (87.4%).

PXRD data (Figure S12) show that the dried material is largely non-crystalline. Adding a drop of water (at t = 0 mins) results in crystallinity being restored, but then largely being lost, which we attribute to the water ordering the material and then slowly evaporating. The PXRD of the rehydrated material is consistent with that calculated from the SCXRD structure.

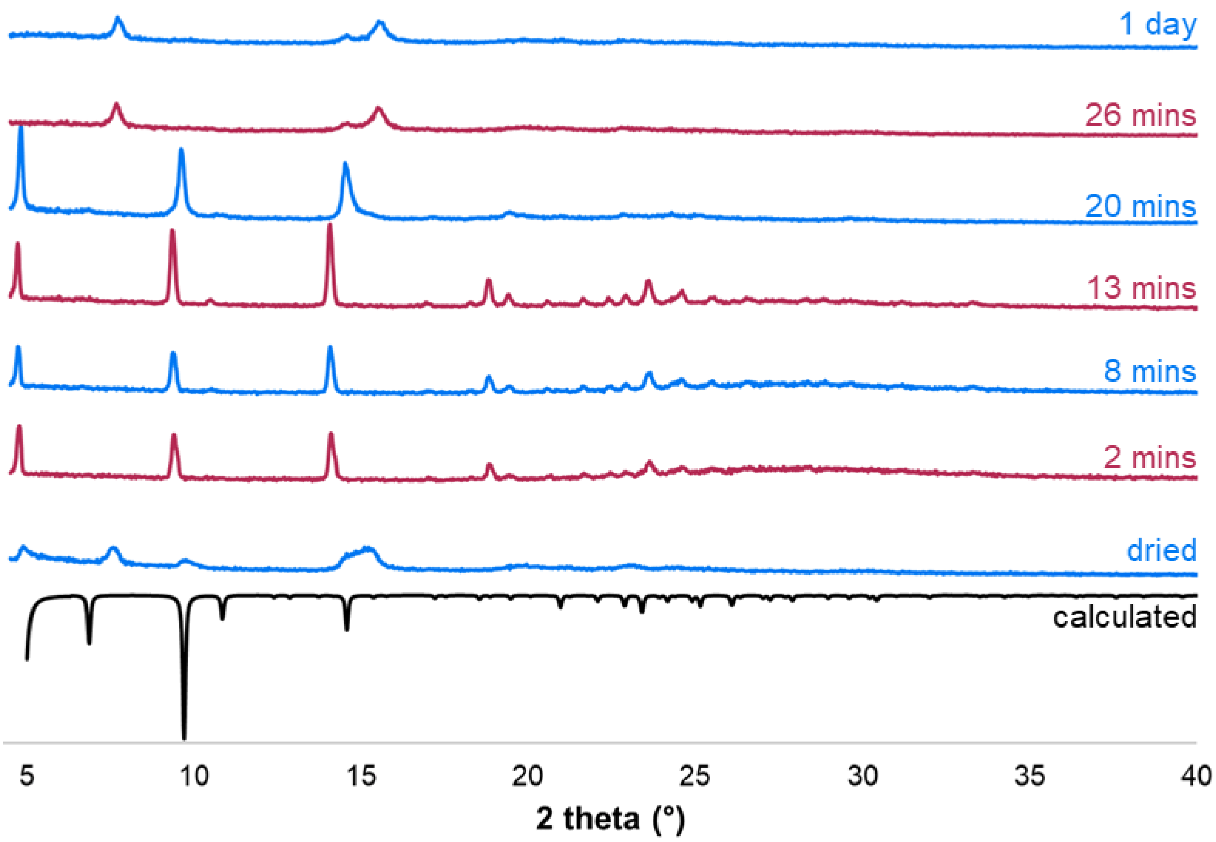

Figure S12. PXRD pattern of **1·DiA**$_2$, and at various times after the addition of water; “calculated” trace represents that predicted from the SCXRD structure.

Studies of *cis*-*trans* isomerisation of DiA^{2-}

A 0.50 mM solution of **K$_2$·DiA** in D_2O was analysed by ^{1}H NMR spectroscopy, which revealed that it was predominantly (> 90%) the *trans* form (Figure S13). The amount of *cis* isomer present before irradiation varied from NMR sample to NMR sample but was always less than 10%. The sample was then exposed to UV-light of 360 nm for 2 hours. Immediately after this, the solution was analysed by ^{1}H NMR spectroscopy, which indicated that 59% had been isomerised to the *cis* form. The percentage of *cis*-**Dia^{2-}** was measured at different time intervals after exposure by comparing the integrations of *trans*-**DiA^{2-}** and *cis*-**DiA^{2-}** peaks, and these data used to plot the isomerisation of the *cis* form back to the *trans* form (Figure S14).

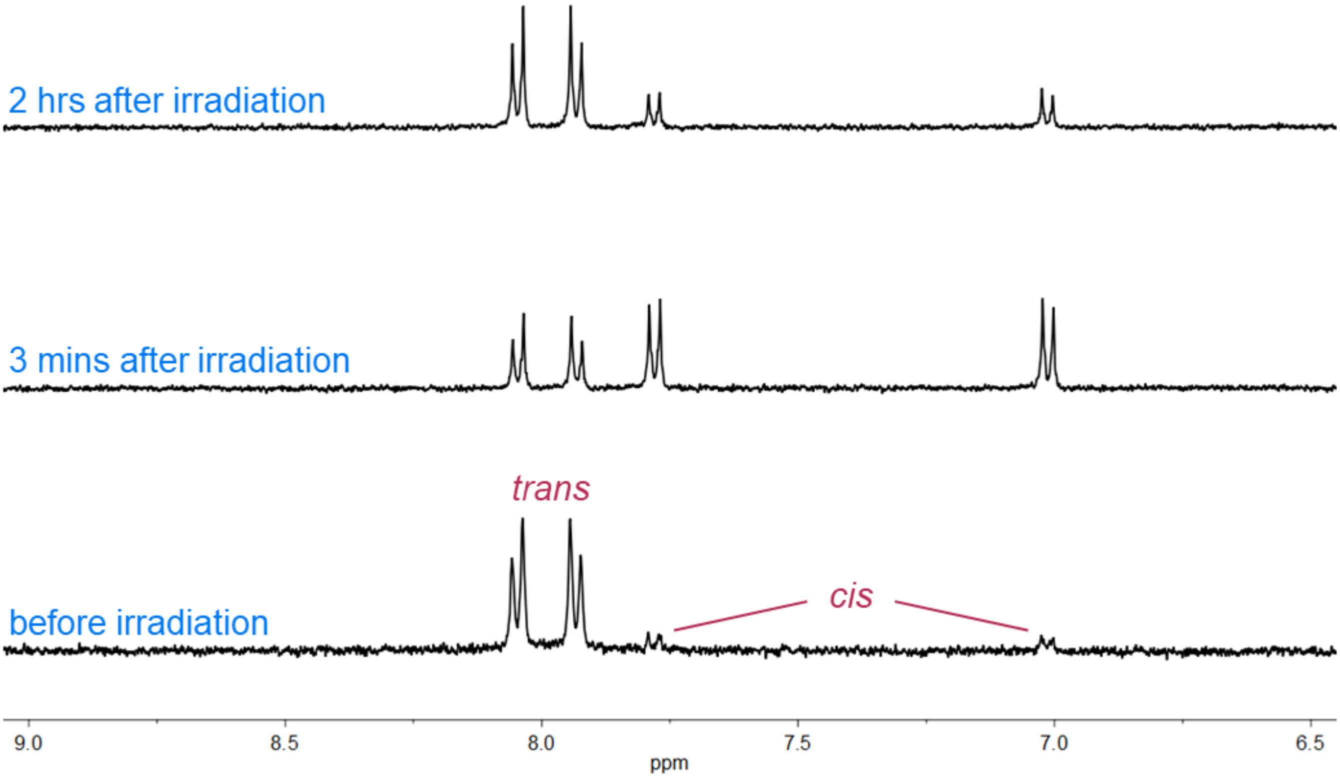

Figure S13. Stacked truncated ^{1}H NMR spectra of **K$_2$·DiA** dissolved in D_2O before and after irradiation with 360 nm light (0.50 mM in D_2O, 400 MHz, 298 K).

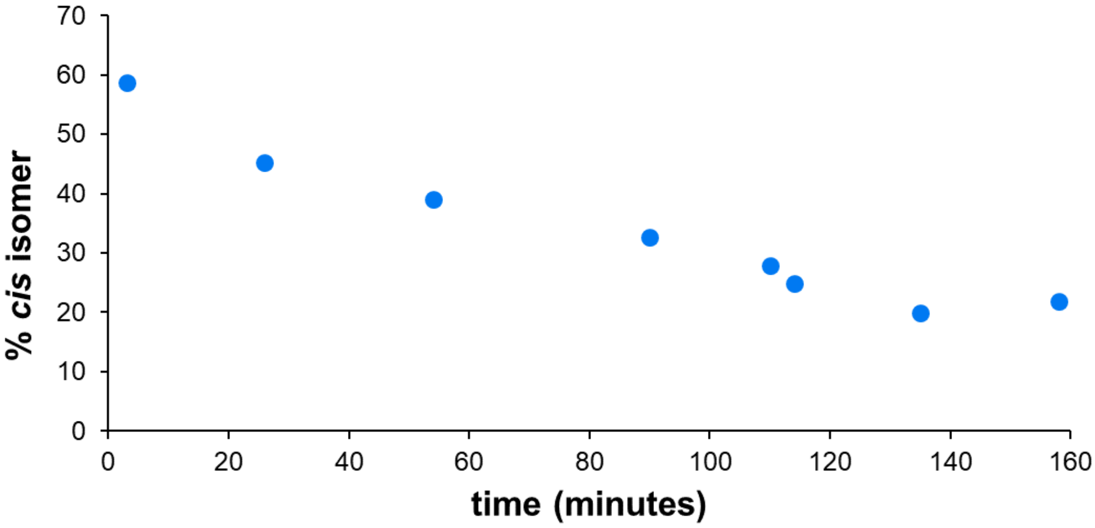

Figure S14. Percentage of *cis*-**DiA^{2-}** at different time intervals after irradiation with 360 nm light (D_2O, 298 K, 0.50 mM).

Crystallisation of $1\cdot DiA_2$ and $1\cdot SB_2$

Reproducibility

It is known that minor changes in conditions such as temperature can have dramatic effects on crystallisation outcomes. To minimise these effects, unless noted below, crystallisations were conducted in at least duplicate, in the same volume of solvent (2 mL) in the same size glass vial (50 × 12 mm) in a climate-controlled laboratory (21−24 °C). Concordant results were obtained in all cases.

Exceptions: Experiments involving irradiating the sample with UV light were all conducted in 10 mL of solvent in75 × 25 mm glass vials. The experiment studying the effect of percentage ethanol in water (0–100%) was only conducted once, although we note that the 0 and 50% ethanol conditions duplicate other crystallisation experiments conducted during the solvent and concentration experiments, and gave concordant results with these.

Crystallisation conditions

The outcome of crystallisations of $\mathbf{1 \cdot DiA_2}$ was very dependent on crystallisation conditions (Table S1). In contrast, $\mathbf{1 \cdot SB_2}$ readily formed mm-long crystals in pure water without the use of modulators (up to 0.50 mM $\mathbf{1}^{4+}$).

Table S1. Outcome of crystallizations of $\mathbf{1 \cdot DiA_2}$.

Solvent	Conc. 1^{4+} (mM)	Additive	Outcome[a]	Time to precipitation
H_2O	0.12	–	✗	< 5 mins
	0.25	–	✗	< 2 mins
	0.50	–	✗	< 1 min
	0.99	–	✗	< 1 min
	1.98	–	✗	< 1 min
50% EtOH[b]	0.14	–	✓	< 20 mins
	0.29	–	✓	< 3 mins
	0.49	–	✓	< 1 min
	1.00	–	✗	< 1 min
	1.98	–	✗	< 1 min
0% EtOH[b]	0.26	–	✗	< 1 min
10% EtOH[b]	0.25	–	✗	< 1 min
20% EtOH[b]	0.27	–	✗	< 1 min
30% EtOH[b]	0.27	–	✗	< 3 mins
40% EtOH[b]	0.26	–	✓	< 3 mins
50% EtOH[b]	0.26	–	✓	< 3 mins
60% EtOH[b]	0.27	–	✓	< 10 min
70% EtOH[b]	0.27	–	✓	< 10 min
80% EtOH[b]	0.26	–	✓	< 10 min
90% EtOH[b]	0.27	–	✓	< 12 hours
H_2O	0.25	9 equiv. NaCl[c]	✗	< 1 min
		26 equiv. NaCl[c]	✗	< 1 min
		36 equiv. NaCl[c]	✗	< 1 min
		84 equiv. NaCl[c]	✗	< 1 min
		100 equiv. NaCl[c]	✗	< 1 min
H_2O	0.25	8 equiv. NaBzO[c]	✗	< 1 min
		19 equiv. NaBzO[c]	✗	< 1 min
		40 equiv. NaBzO[c]	✗	< 1 min
		80 equiv. NaBzO[c]	✗	< 1 min
		102 equiv. NaBzO[c]	✗	< 1 min
H_2O	0.25	9 equiv. Na_2SO_4[c]	✗	< 1 min
		20 equiv. Na_2SO_4[c]	✗	< 1 min
		41 equiv. Na_2SO_4[c]	✗	< 1 min
		80 equiv. Na_2SO_4[c]	✓	< 1 min
		100 equiv. Na_2SO_4[c]	✓	< 1 min
H_2O	0.25	10 equiv. $\mathbf{TBA_2 \cdot NDS}$[c]	✗	< 1 min
		20 equiv. $\mathbf{TBA_2 \cdot NDS}$[c]	✗	< 1 min
		40 equiv. $\mathbf{TBA_2 \cdot NDS}$[c]	✗	< 1 min
		79 equiv. $\mathbf{TBA_2 \cdot NDS}$[c]	✓	< 5 mins
		100 equiv. $\mathbf{TBA_2 \cdot NDS}$[c]	✓	< 5 mins
H_2O	0.25	UV irradiation[d]	✓	< 1 min
50% EtOH[b]	0.25	UV irradiation[d]	✓	< 3 hours

[a] A cross indicates very small crystallites formed, a tick indicates large well-formed crystals were obtained. [b] Volume % EtOH in water. [c] Conducting these experiments using 0.12 mM $\mathbf{1}^{4+}$ gave qualitatively the same results. [d] $\mathbf{DiA}^{2-}$ irradiated at 360 nm for 2 hours before addition of $\mathbf{1}^{4+}$ to induce *trans*-to-*cis* isomerization.

PXRD characterisation of rapidly precipitated 1·DiA$_2$

Rapidly precipitated **1·DiA$_2$** (prepared by mixing aqueous solutions of **1·Cl$_4$** and **K$_2$·DiA**) was thoroughly air-dried for several hours and analysed by PXRD. This dried material is amorphous (Figure S15). Adding a drop of water results in very weak diffraction peaks that rapidly disappear over time.

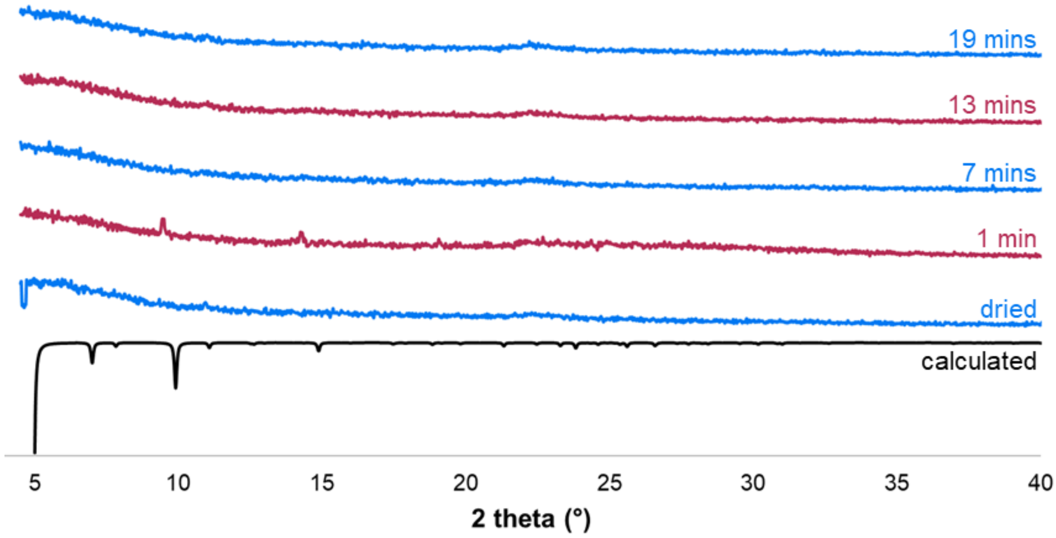

Figure S15. PXRD pattern of thoroughly dried rapidly-precipitated **1·DiA$_2$**, and at various times after the addition of water; "calculated" trace represents that predicted from the SCXRD structure.

If rapidly precipitated **1·DiA$_2$** was prepared in the same manner but was instead air-dried for approximately 15 minutes, *i.e.* not dried thoroughly then this material retains some crystallinity (Figure S16). Adding a drop of water results in increased crystallinity that then disappears over time until the material becomes completely amorphous once all water has evaporated. The PXRD pattern of this is a good match with that calculated from the SCXRD structure of **1·DiA$_2$**, suggesting that the structure of the framework is the same regardless of crystallisation speed and crystal size.

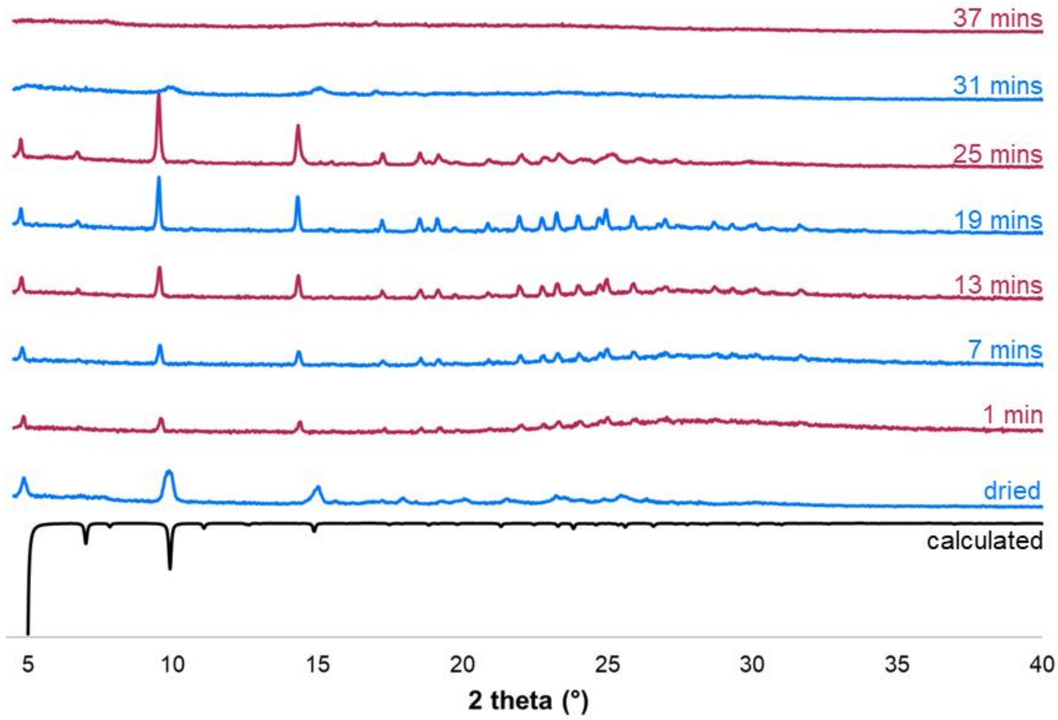

Figure S16. PXRD pattern of partially dried rapidly-precipitated **1·DiA$_2$**, and at various times after the addition of water; "calculated" trace represents that predicted from the SCXRD structure.

Microscopy images of crystals

Effect of modulators: Pictures of crystals grown under various conditions are provided in Figures S17–S19. As shown in Figure S17, benzoate seemed to have little effect as a modulator, with rapid precipitation of very small crystals occurring even in the presence of 100 equivalents of sodium benzoate. Chloride seems to have a limited effect, with crystallisation slowed slightly and slightly larger crystals forming when 100 equivalents of sodium chloride were used. In contrast, both sodium sulfate (Figure S18) and **TBA_2·NDS** (Figure S19) are effective modulators, with relatively large crystals being formed in the presence of large equivalents of modulator and the size of crystals increasing with increasing amount of modulator used. While smaller crystals appear colourless in some of the images in Figures S17–S19, by eye all crystals were orange.

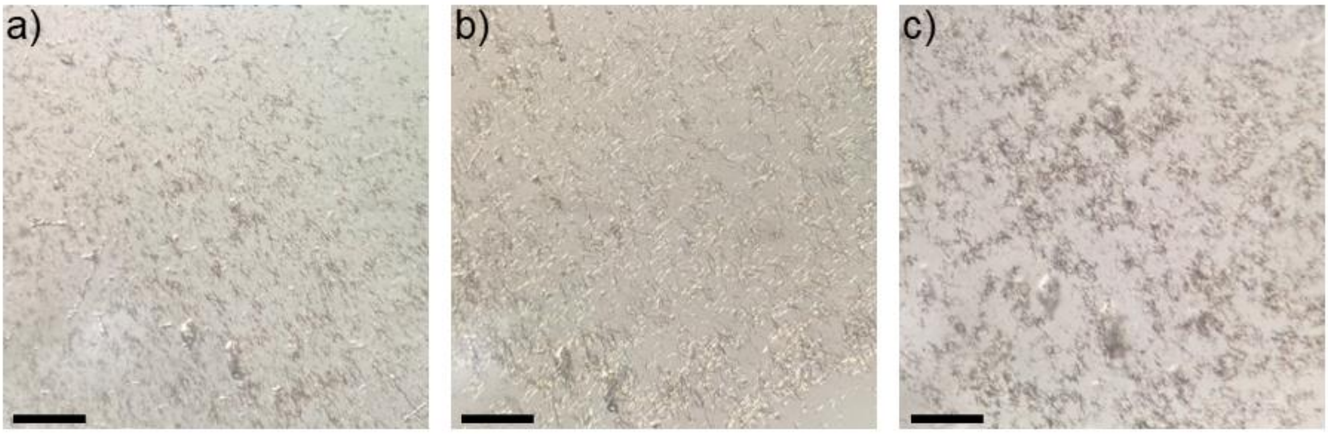

Figure S17. Optical microscope images of crystals of **1·DiA_2** grown under various conditions: a) 0.25 mM **1^{4+}** in H_2O no modulator; b) 0.25 mM **1^{4+}** in H_2O, 100 equivalents NaCl; c) 0.25 mM **1^{4+}** in H_2O, 100 equivalents sodium benzoate (scale bar represents 1 mm in all images).

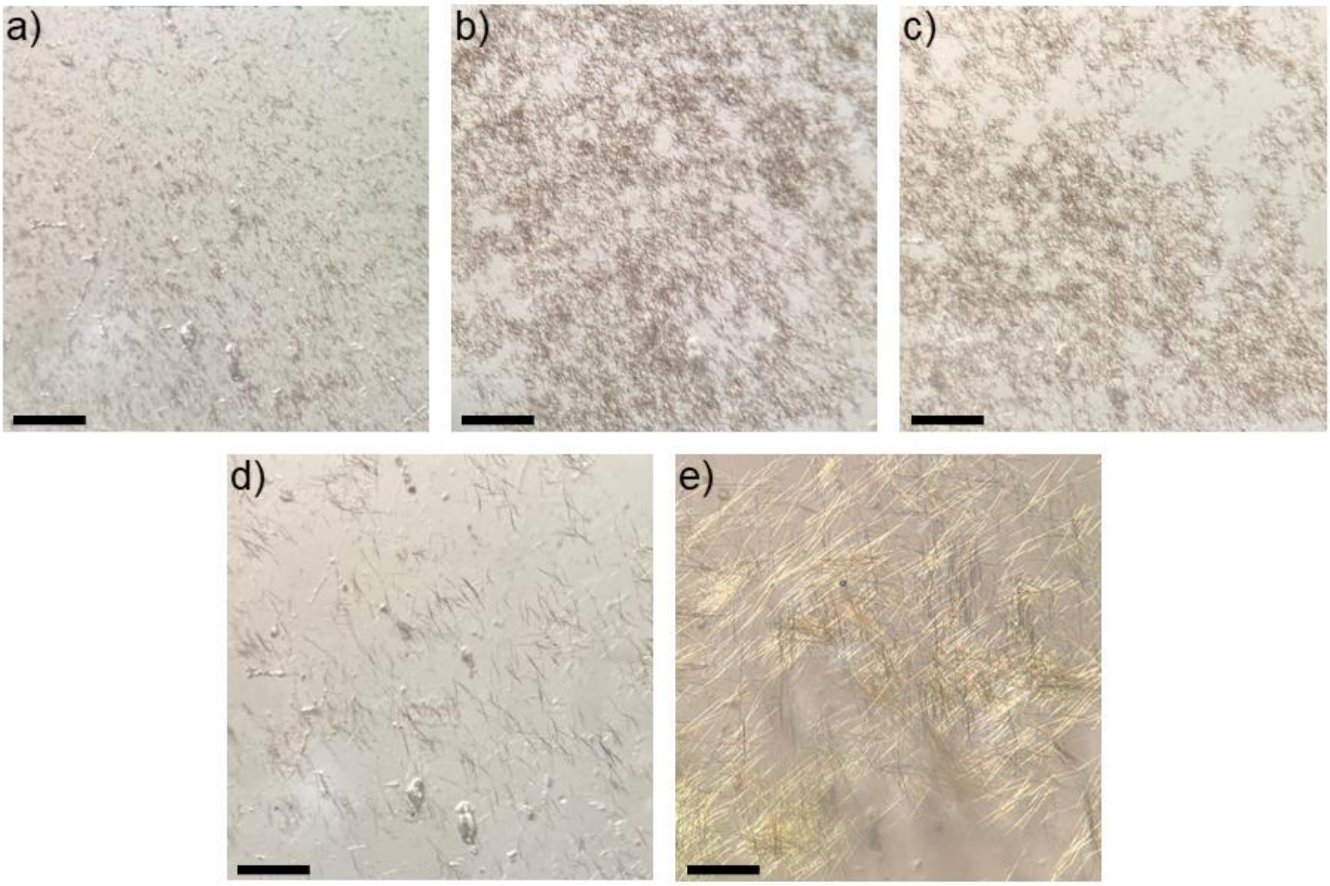

Figure S18. Optical microscope images of crystals of **1·DiA_2** grown in the presence of various numbers of equivalents of Na_2SO_4: a) 0 equivalents; b) 10 equivalents; c) 20 equivalents; d) 40 equivalents; e) 100 equivalents (all crystallisations conducted with 0.25 mM **1^{4+}** in H_2O, scale bar represents 1 mm in all images).

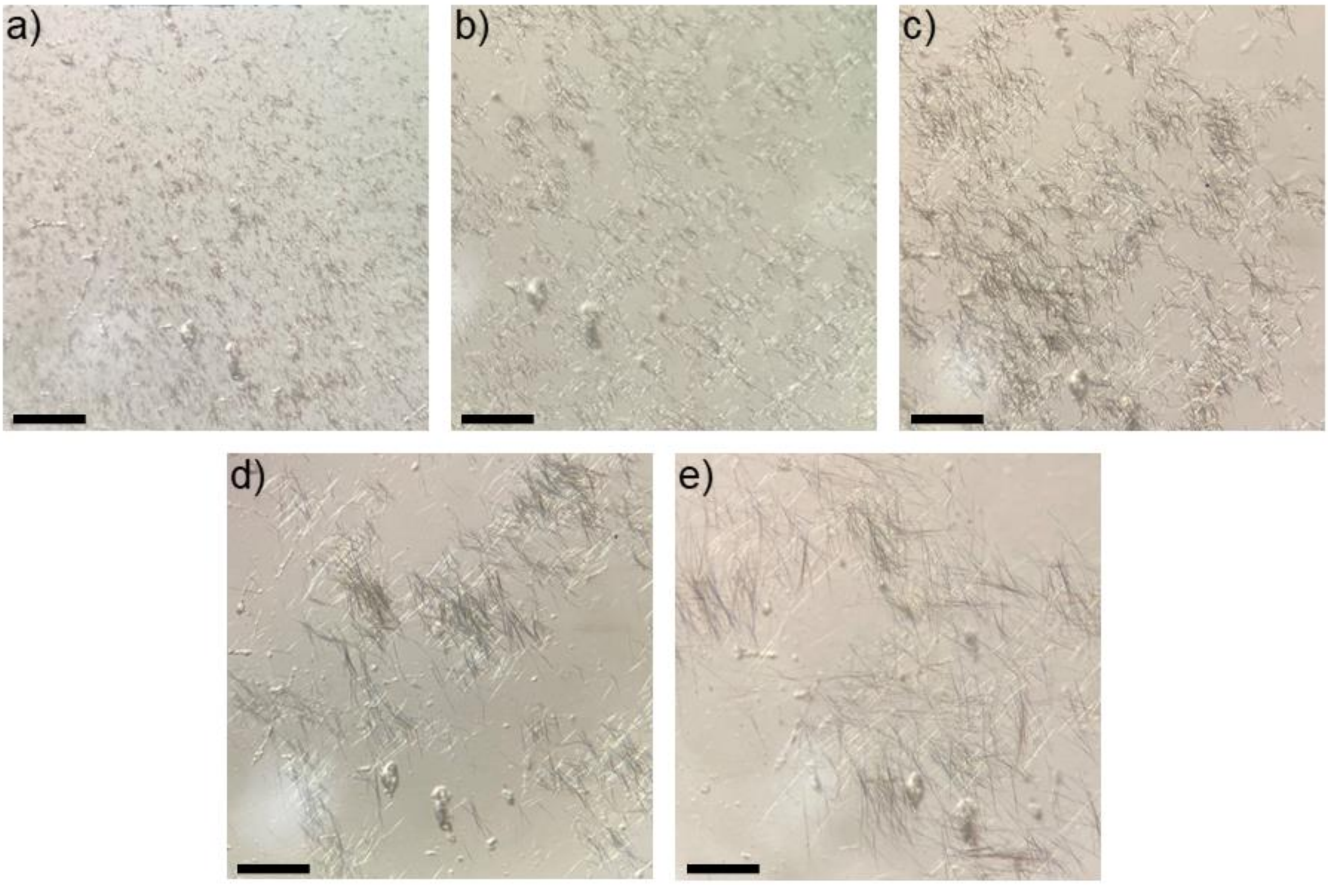

Figure S19. Optical microscope images of crystals of **1·DiA$_2$** grown in the presence of various numbers of equivalents of **TBA$_2$·NDS**: a) 0 equivalents; b) 10 equivalents; c) 20 equivalents; d) 40 equivalents; e) 100 equivalents (all crystallisations conducted with 0.25 mM **1**$^{4+}$ in H_2O, scale bar represents 1 mm in all images).

Effect of UV light, H_2O: Pictures of crystals grown by simply mixing **1·Cl$_4$** and **K$_2$·DiA** in water and crystals grown in an analogous experiment where the solution of **K$_2$·DiA** was first irradiated with UV light (λ = 360 nm) are compared in Figure S20.

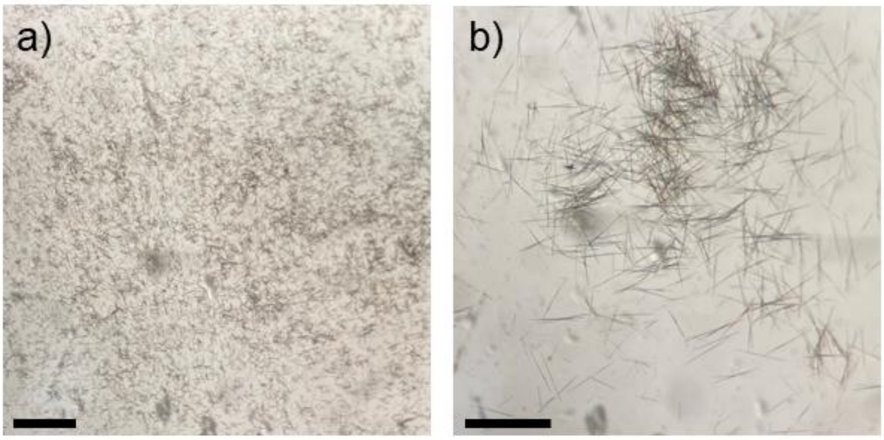

Figure S20. Optical microscope images of crystals of **1·DiA$_2$** grown either without irradiating **K$_2$·DiA** with UV light (a), or with prior irradiation with UV light (b) (crystallisations conducted with 0.25 mM **1**$^{4+}$ in H_2O, scale bar represents 1 mm in both images).

Effect of UV light, 1:1 H_2O:EtOH: Pictures of crystals grown by simply mixing **1·Cl$_4$** and **K$_2$·DiA** in 1:1 water:ethanol and crystals grown in an analogous experiment where the solution of **K$_2$·DiA** was first irradiated with UV light (λ = 360 nm) are compared in Figure S21.

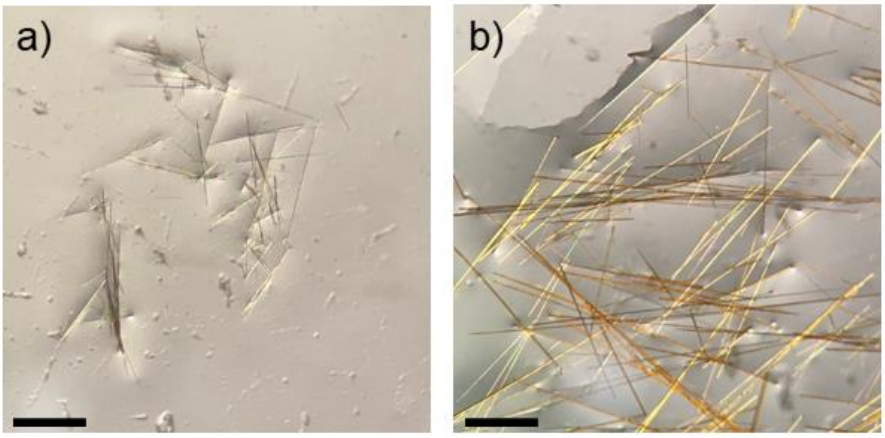

Figure S21. Optical microscope images of crystals of **1·DiA$_2$** grown either without irradiating **K$_2$·DiA** with UV light (a), or with prior irradiation with UV light (b) (crystallisations conducted with 0.25 mM **1**$^{4+}$ in 1:1 H_2O:ethanol, scale bar represents 1 mm in both images).

Crystals of 1·SB$_2$: Very large crystals of **1·SB$_2$** formed from either water or 1:1 H_2O:EtOH without the need for any modulators (Figure S22).

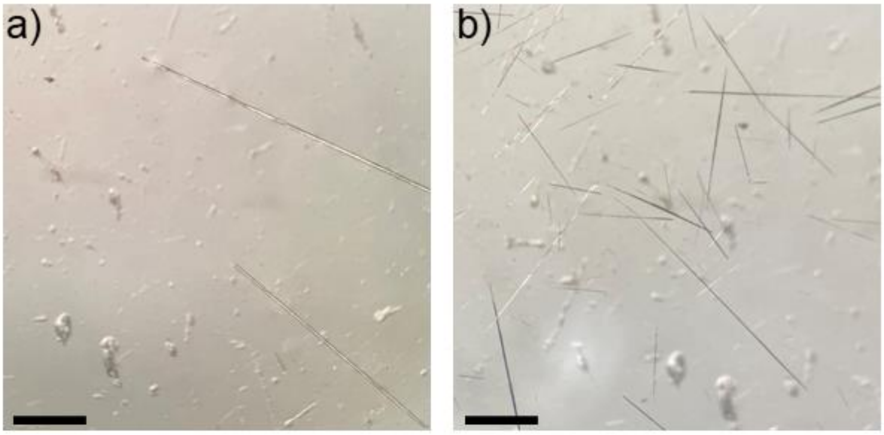

Figure S22. Optical microscope images of crystals of **1·SB$_2$** grown in either a) H_2O or b) 1:1 H_2O:EtOH (both crystallisations conducted with 0.25 mM **1**$^{4+}$ without modulators, scale bar represents 1 mm in both images).

Scanning electron microscopy images of crystals

Scanning electron microscopy images of crystals grown in the presence of 0, 10 or 100 equivalents of Na_2SO_4 (0.25 mM of $\mathbf{1}^{4+}$ in H_2O) are provided at different magnifications in Figures S23–S25.

No modulator:

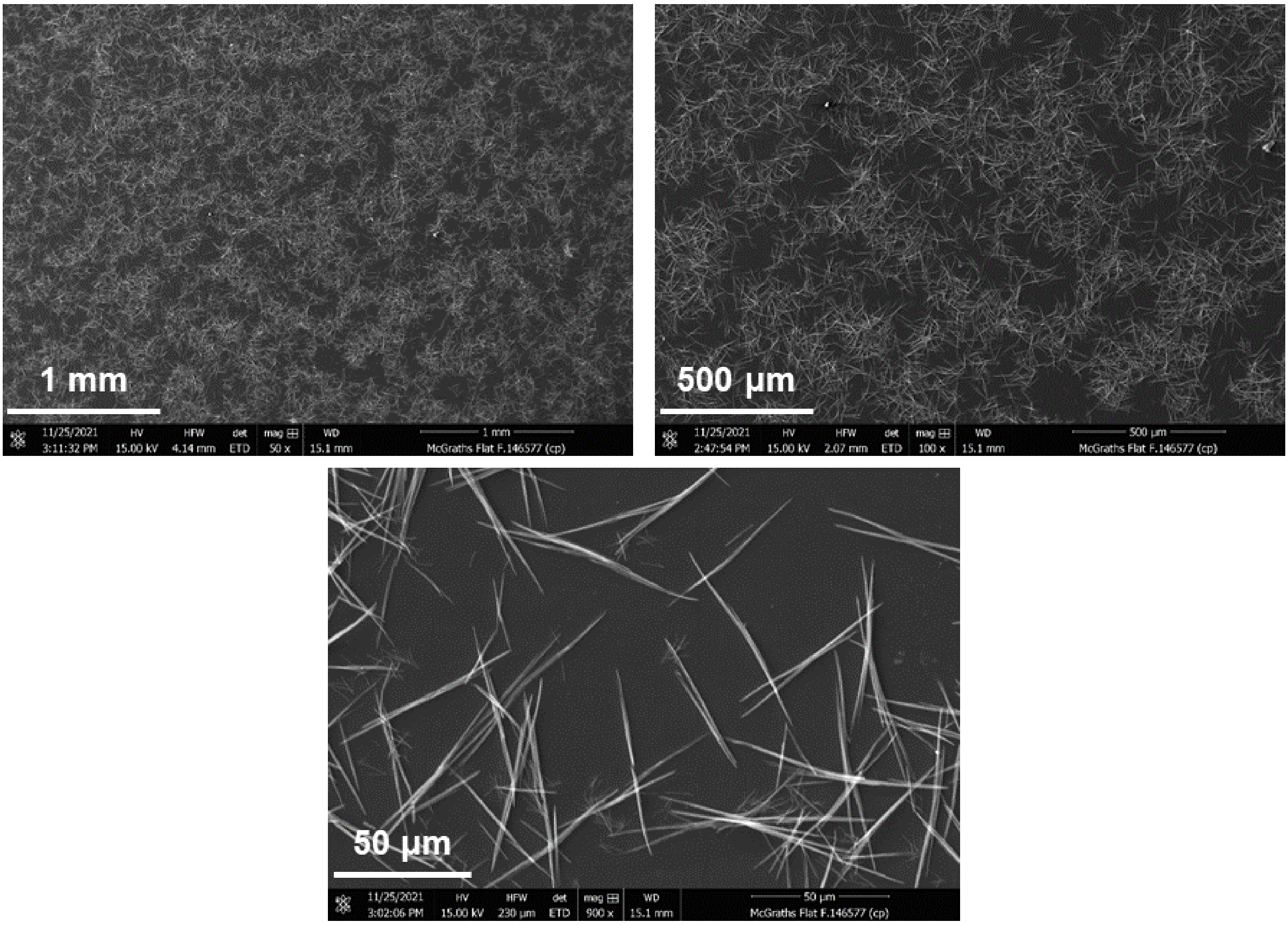

Figure S23. SEM images of crystals of **1·DiA₂** grown without modulator (0.25 mM of $\mathbf{1}^{4+}$, H_2O). Small scale bars are present at the bottom right of the images, but have been reproduced in larger font (white) for ease of viewing.

10 equiv. Na_2SO_4:

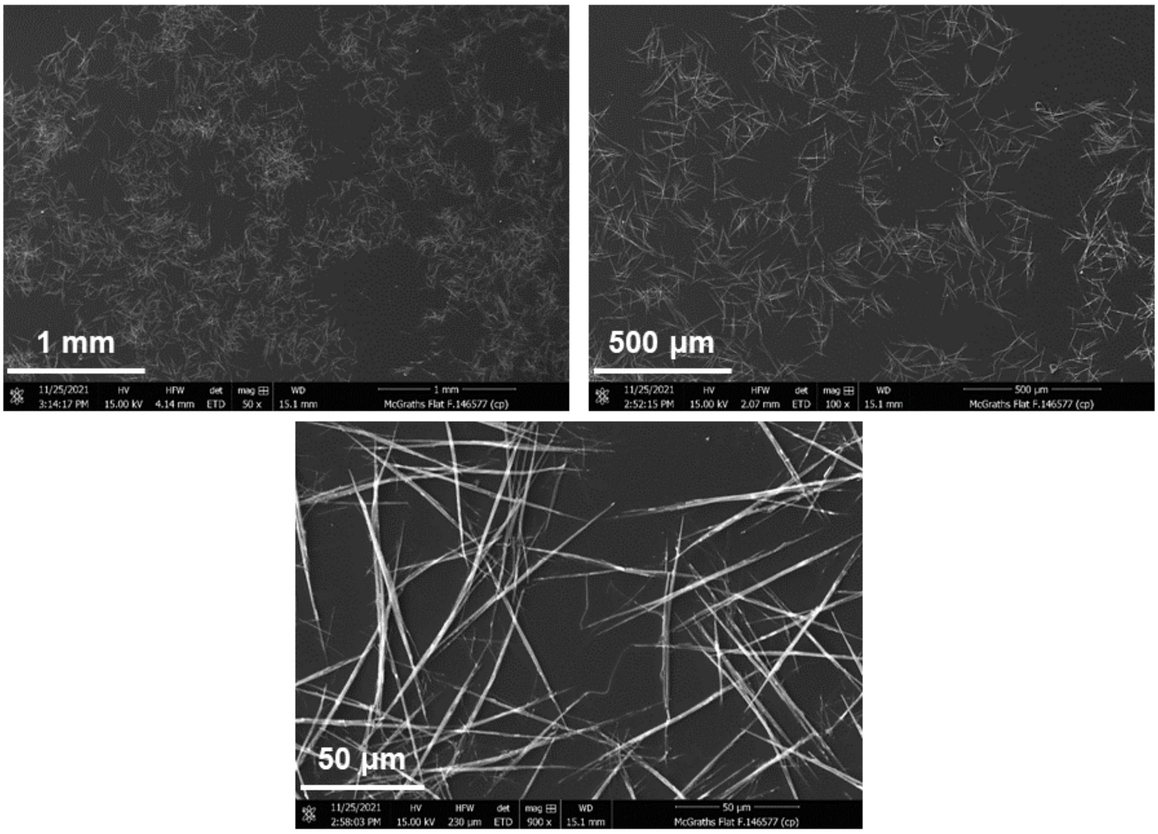

Figure S24. SEM images of crystals of **1·DiA$_2$** grown in the presence of 10 equivalents of Na_2SO_4 (0.25 mM of **1^{4+}**, H_2O). Small scale bars are present at the bottom right of the images, but have been reproduced in larger font (white) for ease of viewing.

100 equiv. Na_2SO_4:

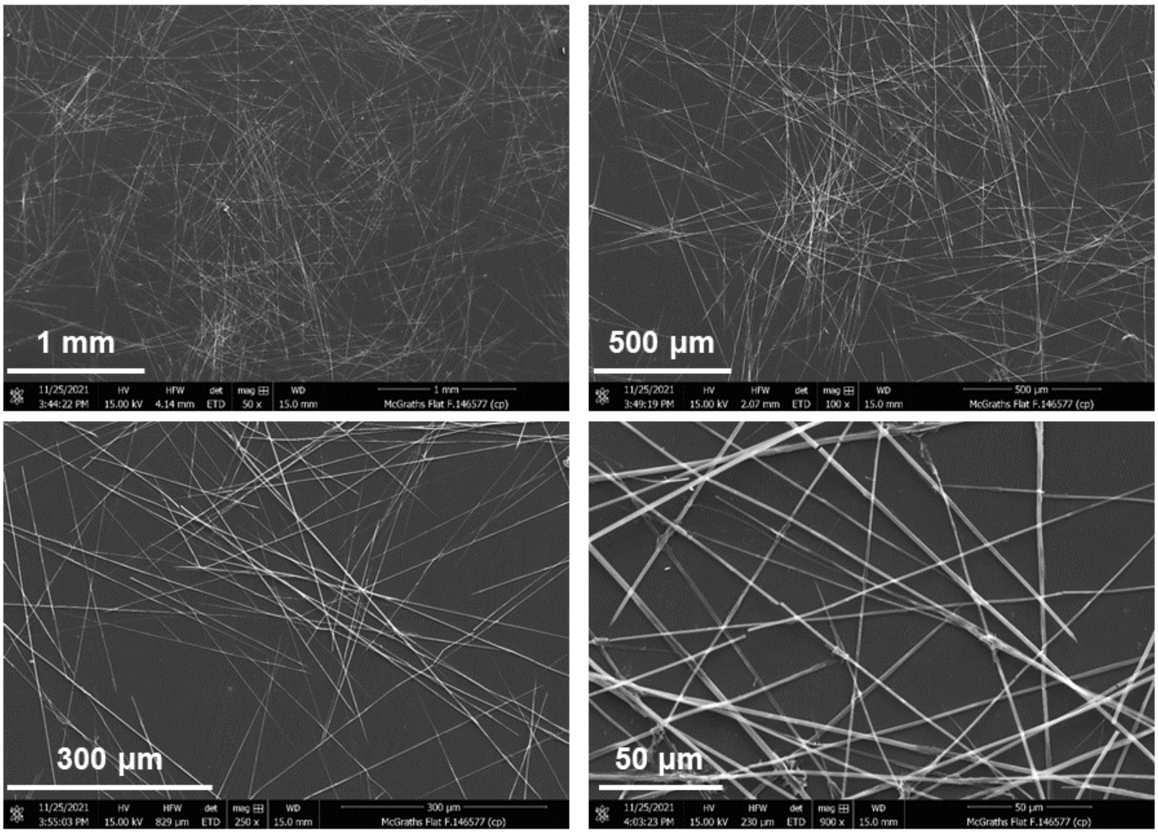

Figure S25. SEM images of crystals of **1·DiA$_2$** grown in the presence of 100 equivalents of Na_2SO_4 (0.25 mM of **1^{4+}**, H_2O). Small scale bars are present at the bottom right of the images, but have been reproduced in larger font (white) for ease of viewing.

Size distribution of crystals grown in the presence of Na_2SO_4

Size distributions were calculated from backscattered SEM images of crystals grown in the presence of various numbers of equivalents of Na_2SO_4. Well isolated and resolved crystals were measured using ImageJ.

Crystal length:

Crystal length data are presented in Table S2 and Figure S26. Statistically significant ($p < 0.0001$) increases in the mean crystal length are observed for increasing equivalents of Na_2SO_4.

Table S2. Crystal lengths (all values in μm).

	0 equiv. Na_2SO_4[a]	**10 equiv. Na_2SO_4[a]**	**100 equiv. Na_2SO_4[a]**
Minimum length	33	43	277
Maximum length	67	158	1357
Number of crystals measured	48	27	32
Mean length	**48**	**102**	**695**
Estimated SE of mean[b]	1.1	4.5	45
95% CI of mean	**45 – 51**	**92 – 111**	**604 – 785**

[a] Crystals grown in water (0.25 mM of **1^{4+}**) and varying number of equivalents of Na_2SO_4. [b] Estimated as $\sigma/\sqrt{N}$.

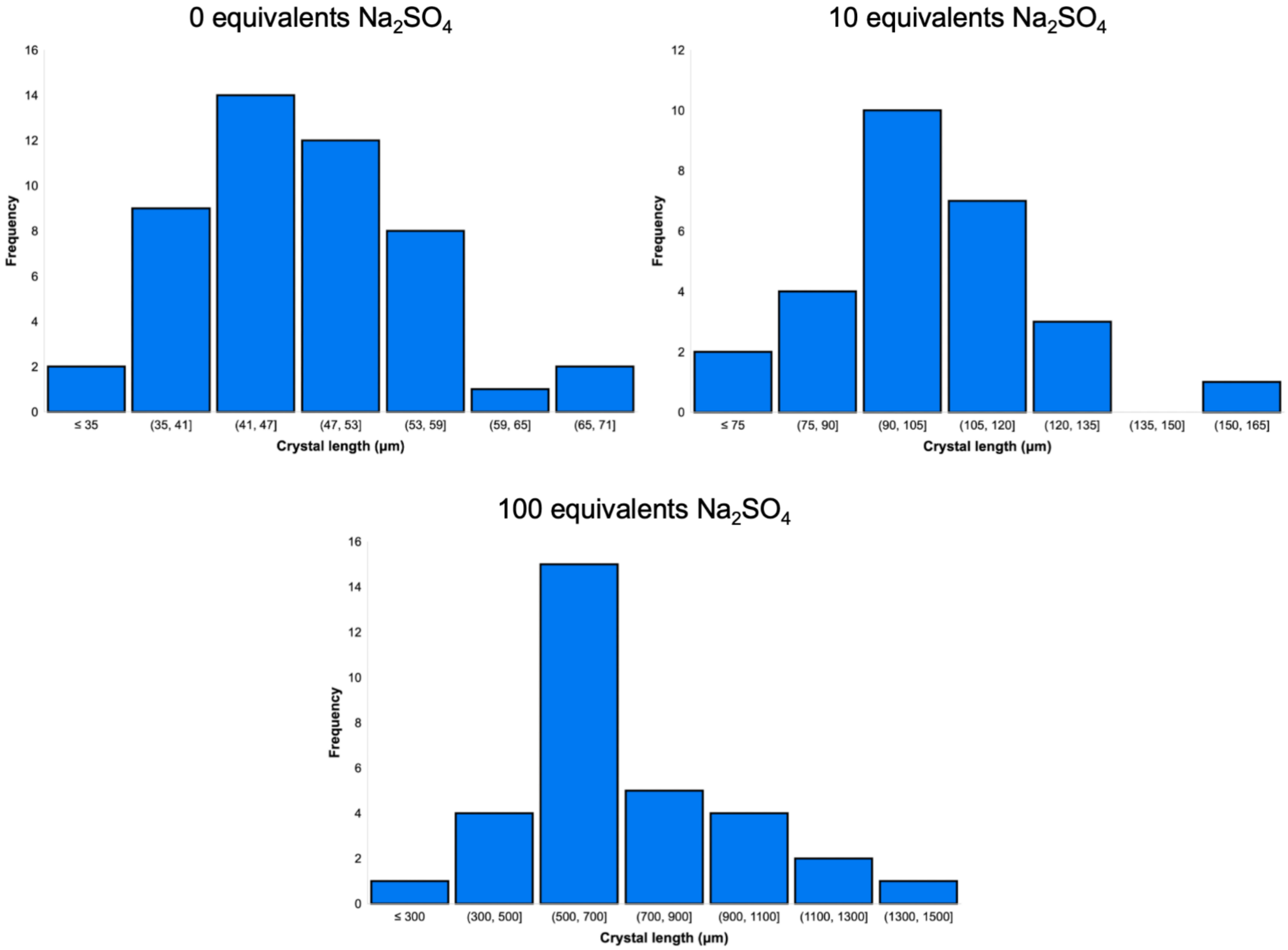

Figure S26. Histograms showing the length of crystals of **1·DiA$_2$** grown in the presence of 0, 10 or 100 equivalents of Na_2SO_4 (0.25 mM **1^{4+}** in H_2O). *Note that different scales are used for each histogram*.

Crystal diameter:

Crystal diameter data are presented in Table S3 and Figure S27. There is no significant difference in the means of the diameters of crystals grown in the presence of 0 or 10 equivalents of Na_2SO_4, but a statistically significant difference between either of these values and the mean diameter for crystals grown in the presence of 100 equivalents of Na_2SO_4 ($p < 0.0001$).

Table S3. Crystal diameters (all values in μm).

	0 equiv. Na_2SO_4[a]	**10 equiv. Na_2SO_4[a]**	**100 equiv. Na_2SO_4[a]**
Minimum diameter	0.88	0.61	0.90
Maximum diameter	2.85	3.05	3.64
Number of crystals measured	29	38	42
Mean diameter	**1.34**	**1.31**	**2.17**
Estimated SE of mean[b]	0.08	0.08	0.09
95% CI of mean	**1.17 – 1.51**	**1.16 – 1.47**	**2.00 – 2.34**

[a] Crystals grown in water (0.25 mM of **1**$^{4+}$) and varying number of equivalents of Na_2SO_4. [b] Estimated as $\sigma/\sqrt{N}$.

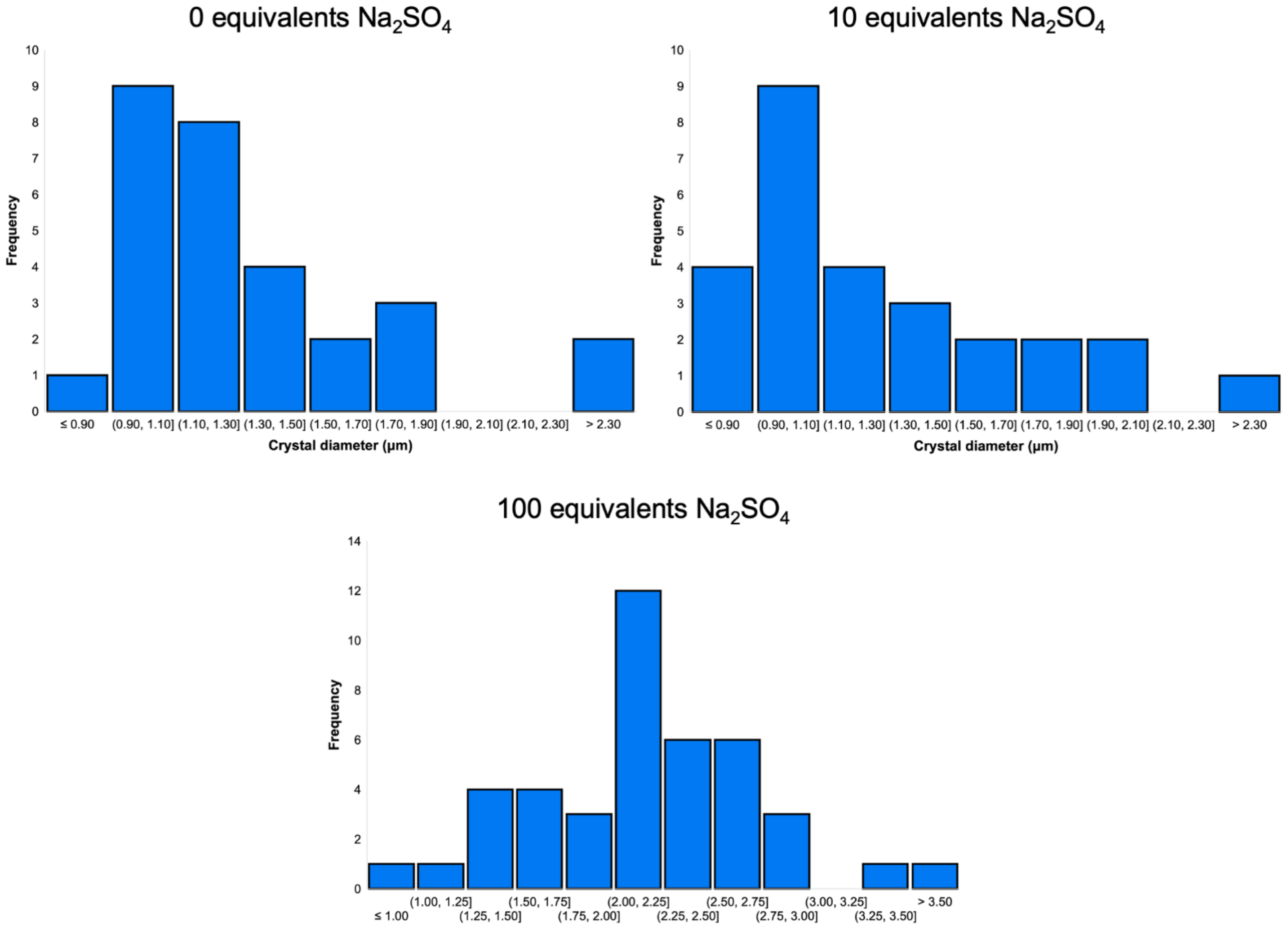

Figure S27. Histograms showing the diameter of crystals of **1·DiA₂** grown in the presence of 0, 10 or 100 equivalents of Na_2SO_4 (0.25 mM **1**$^{4+}$ in H_2O). *Note that a different scale is used for the histogram for 100 equivalents, but the histograms for 0 and 10 equivalents use the same scale.*

Single crystal X-ray crystallography (SCXRD)

Data collection and refinement

Data for **T·DiA$_2$** and **T·SB$_2$** were collected on the MX2 beamline[2] at the Australian Synchrotron at 100 K. Raw frame data (including data reduction, interframe scaling and unit cell refinement) were processed using XDS.[3] Structures were solved using SHELXS[4] and refined using SHELXL[5] within the OLEX2 suite.[6]

The two structures are isostructural, both crystallising in the tetragonal space group $P4_2/n$, with one quarter of a tetraamidinium cation and one half of a dicarboxylate anion in the asymmetric unit. Initial data collections of both structures on a home-source diffractometer revealed that crystals were twinned and that there were large void spaces containing diffuse electron density that appeared to arise from poorly defined partial occupancy water molecules. Data were collected on a home source for four crystals of **T·DiA$_2$** and two crystals of **T·SB$_2$** — while the quality of the data varied, all were twinned (appropriate twin laws were found and implemented within OLEX2 for the refinements described herein[6]), and all had similarly poorly resolved solvent molecules in the void.

In an effort to overcome some of these issues, crystals were mounted at 213 K using a 3D-printed *µ*CHILL cold mounting device.[7] The crystals were immediately submerged in liquid nitrogen and transferred to the Australian Synchrotron using a dry shipper. Crystals were kept in liquid nitrogen until use. Despite these precautions, there is relatively little electron density located in the voids, suggesting loss of solvent. It was possible to model the solvent as partial occupancy water molecules, but this required the use of strict ISOR restraints and led to a relatively poor quality refinement of both structures and it was not possible to locate the hydrogen atoms for these water molecules. Briefly, the refinements suggested 11–12 sites for water molecules with a total occupancy of 5–7 per asymmetric unit, and gave R_1 [$I>2\sigma(I)$] values of ~ 10%, and wR2 (all) values of ~ 26–28%. Significantly higher quality refinements were obtained by using PLATON-SQUEEZE[8] to incorporate diffuse electron density (see Table S4 for refinement data). In the structure of **T·DiA$_2$**, PLATON-SQUEEZE[8] removed 1073 electrons from a void with a solvent accessible volume of 2544 Å^3 (54% of the unit cell), while in the structure of **T·SB$_2$**, PLATON-SQUEEZE[8] removed 727 electrons from a void with a solvent accessible volume of 2673 Å^3 (54% of the unit cell)

After incorporation of the solvent electron density in the model using PLATON-SQUEEZE[8] refinement proceeded smoothly. In both structures, the tetraamidinium part of the structure is very well-behaved and has small and approximately spherical ellipsoids. In both structures, the dicarboxylate anion has larger ellipsoids and these are elongated in one direction (at 90° to the axis of the molecule). In the case of **SB^{2-}**, the bond lengths and angles refined to sensible values without the use of restraints. In the case of **DiA^{2-}**, it was necessary to use relatively strict DFIX, DANG, DELU and SIMU restrains on the dianion to achieve a chemically sensible refinement. We attempted to model the anion split over two positions, but were unable to achieve a chemically sensible refinement in this manner. While there is some motion associated with the dicarboxylate anions, the overall chemical structure of both frameworks can be determined unambiguously from the data.

Full crystallographic data in CIF format are provided as Supporting Information (CCDC Numbers: 2118273 and 2118274). Selected data are summarised in Table S4.

Table S4. Selected crystallographic data.

Compound	**1·DiA$_2$** [a]	**1·SB$_2$** [a]
Radiation type	synchrotron (λ = 0.71075 Å)	synchrotron (λ = 0.71075 Å)
Temperature (K)	100	100
Formula	$C_{29}H_{32}N_8 \cdot (C_{14}H_8N_2O_4)_2 \cdot$ *solvents*[a]	$C_{29}H_{32}N_8 \cdot (C_{16}H_{10}O_4)_2 \cdot$ *solvents*[a]
Formula weight	1029.07	1025.10
a (Å)	25.440(4)	25.779(4)
b (Å)	25.440(4)	25.779(4)
c (Å)	7.3400(15)	7.4300(15)
α (º)	90	90
β (º)	90	90
γ (º)	90	90
Unit cell volume (Å^3)	4750.4(17)	4937.7(17)
Crystal system	tetragonal	tetragonal
Space group	$P4_2$/n	$P4_2$/n
Z	2	2
Reflections (all)	64383	65639
Reflections (unique)	4758	4846
R_{int}	0.082	0.088
R_1 [$I > 2\sigma(I)$]	0.056	0.065
wR_2 (all data)	0.181	0.193
CCDC number	2118273	2118274

[a] PLATON SQUEEZE[8] used.

Additional pictures of the structure of 1·DiA₂

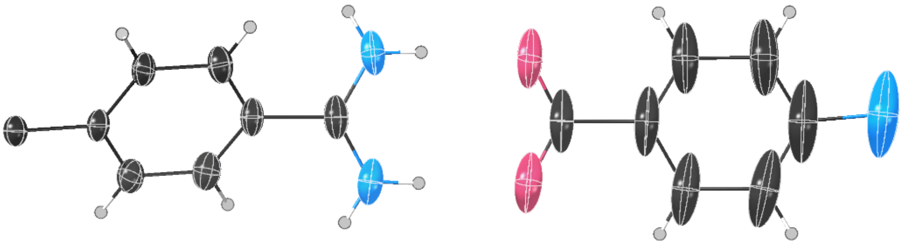

Figure S28. Thermal ellipsoid plot showing the asymmetric unit of **1·DiA₂**; ellipsoids shown at 50% probability level, PLATON-SQUEEZE[8] used.

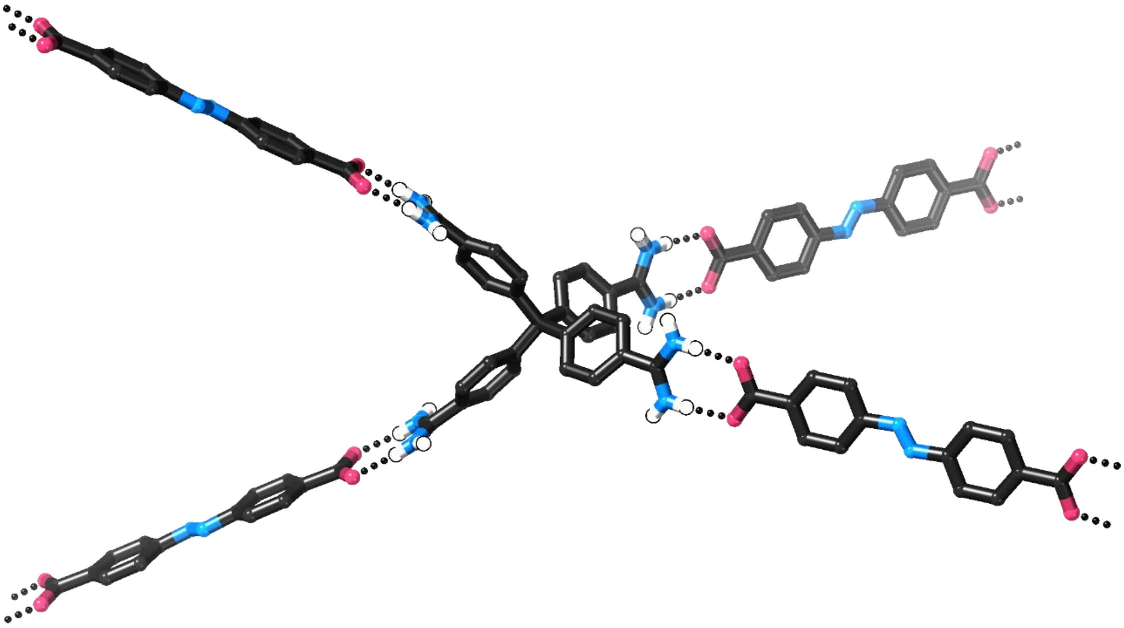

Figure S29. Diagram showing the H-bonding interactions in the structure of **1·DiA₂**.

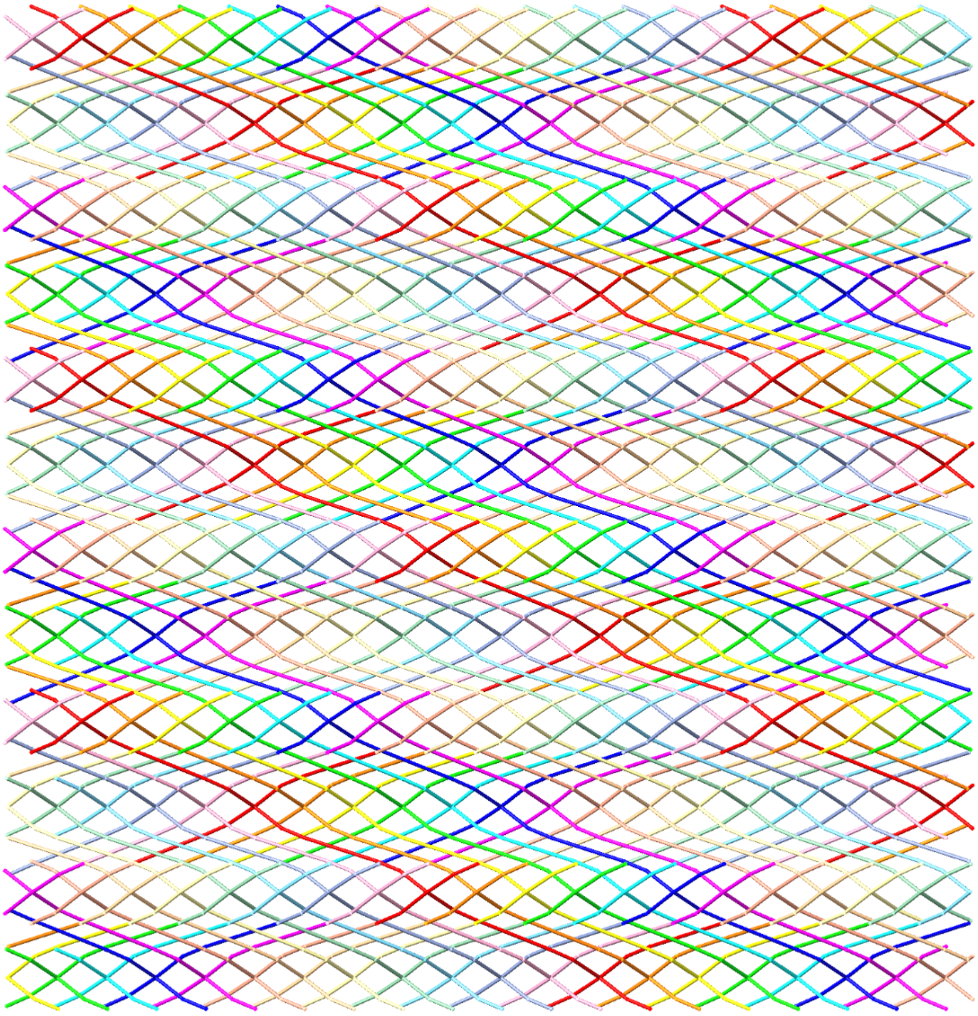

Figure S30. Diagram showing the 14 interpenetrated diamondoid networks in **1·DiA₂**. Each network is simplified by only showing the amidinium and carboxylate carbon atoms as well as the central sp^3 carbon atom (C3, C10 and C13 in the CIF), with each distinct network shown in a different colour.

Pictures of the structure of 1·SB₂

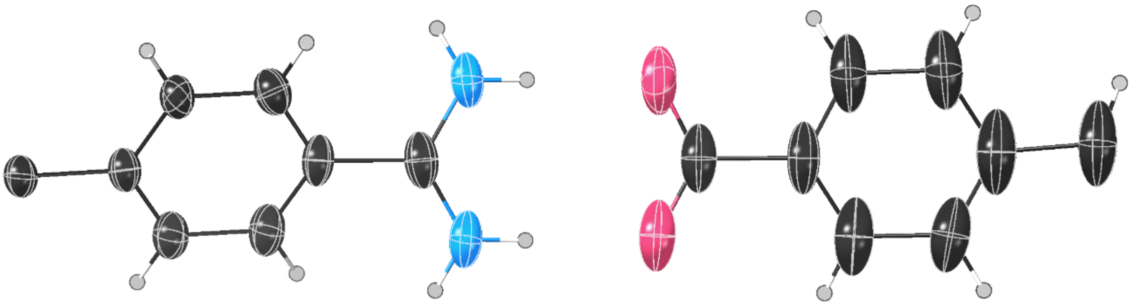

Figure S31. Thermal ellipsoid plot showing the asymmetric unit of **T·SB₂**; ellipsoids shown at 50% probability level, PLATON-SQUEEZE[8] used.

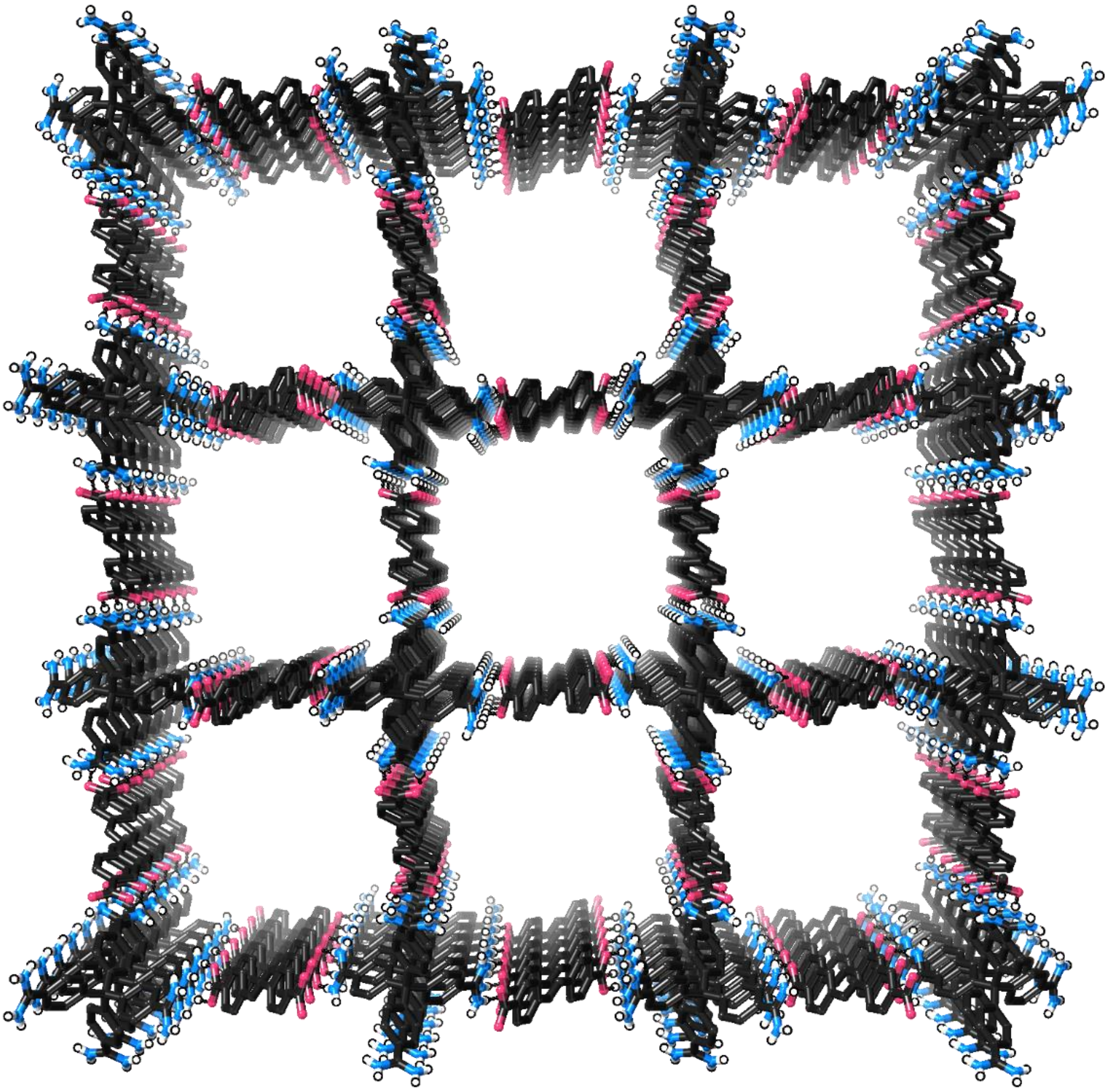

Figure S32. Single crystal structure of **1·SB₂**; most hydrogen atoms are omitted for clarity, PLATON-SQUEEZE[8] used.

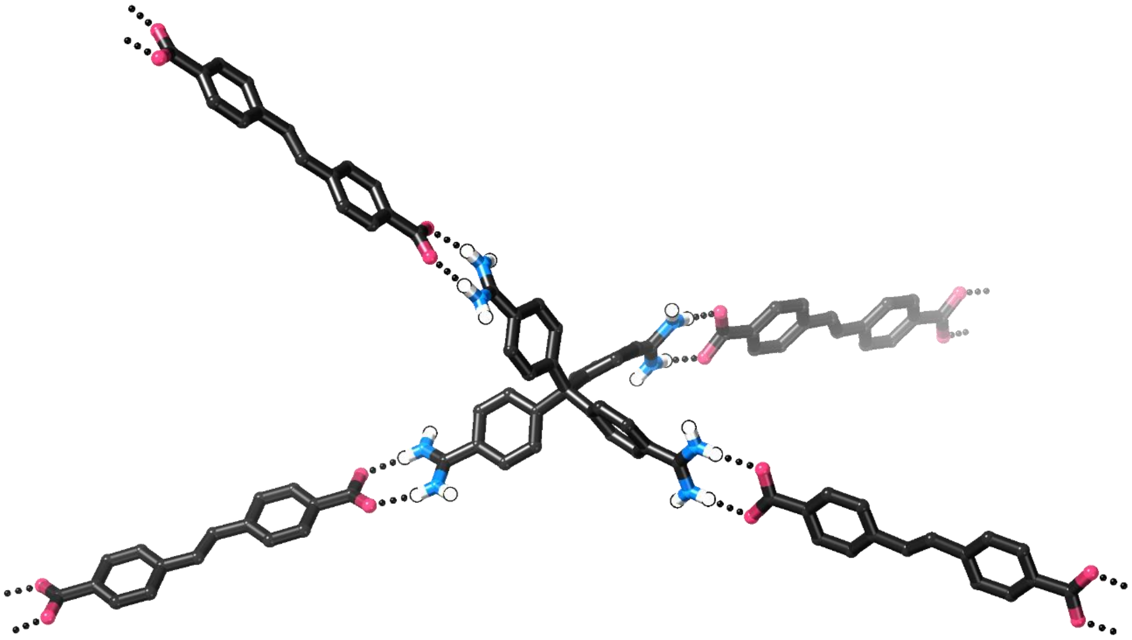

Figure S33. Diagram showing the H-bonding interactions in the structure of **1·SB₂**.

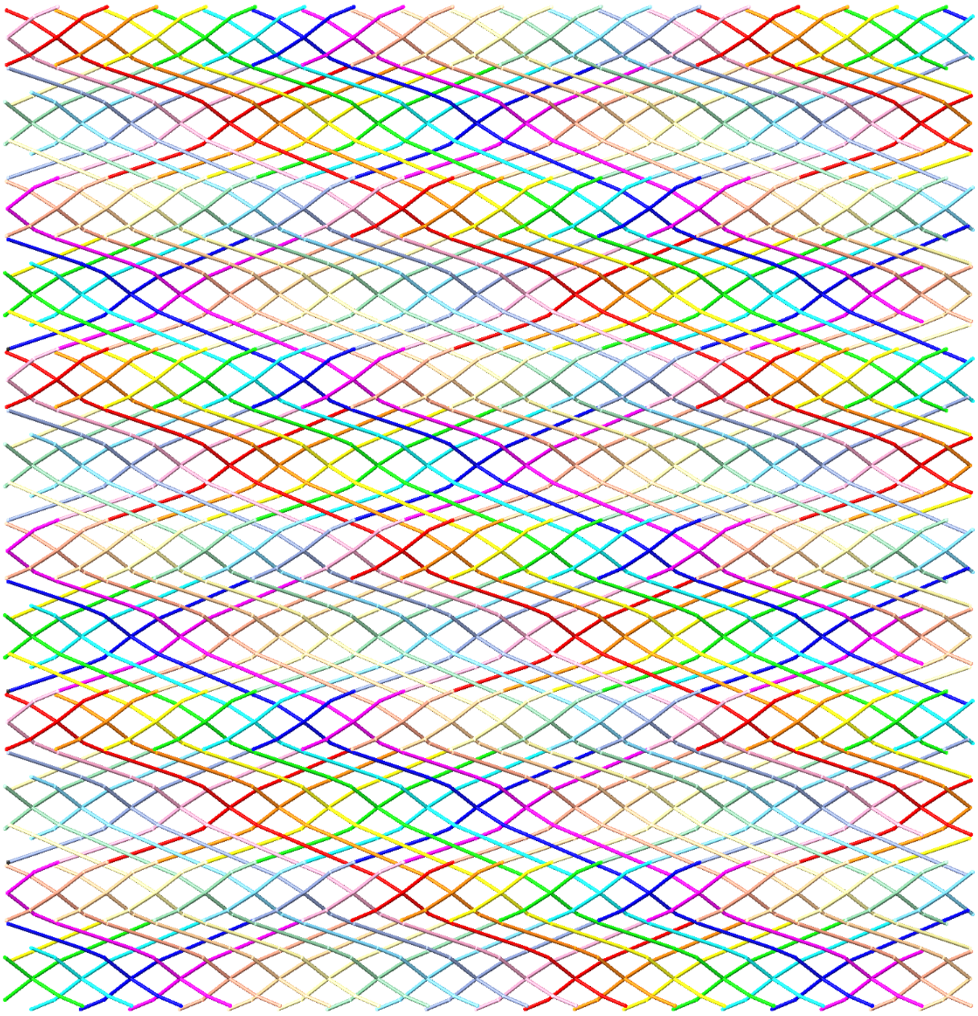

Figure S34. Diagram showing the 14 interpenetrated diamondoid networks in **1·SB₂**. Each network is simplified by only showing the amidinium and carboxylate carbon atoms as well as the central sp^3 carbon atom (C3, C10 and C13 in the CIF), with each distinct network shown in a different colour.

References

1. M. Morshedi, M. Thomas, A. Tarzia, C. J. Doonan and N. G. White, Supramolecular anion recognition in water: synthesis of hydrogen-bonded supramolecular frameworks, *Chem. Sci.* **2017**, *8*, 3019–3025.
2. D. Aragao, J. Aishima, H. Cherukuvada, R. Clarken, M. Clift, N. P. Cowieson, D. J. Ericsson, C. L. Gee, S. Macedo, N. Mudie, S. Panjikar, J. R. Price, A. Riboldi-Tunnicliffe, R. Rostan, R. Williamson and T. T. Caradoc-Davies, MX2: a high-flux undulator microfocus beamline serving both the chemical and macromolecular crystallography communities at the Australian Synchrotron, *J. Synchrotron Radiat.* **2018**, *25*, 885–891.
3. W. Kabsch, Automatic processing of rotation diffraction data from crystals of initially unknown symmetry and cell constants, *J. Appl. Crystallogr.* **1993**, *26*, 795–800.
4. G. M. Sheldrick, A short history of SHELX, *Acta Crystallogr.* **2008**, *A64*, 112–122.
5. G. M. Sheldrick, Crystal structure refinement with SHELXL, *Acta Crystallogr.* **2015**, *C71*, 3–8.
6. O. V. Dolomanov, L. J. Bourhis, R. J. Gildea, J. A. K. Howard and H. Puschmann, OLEX2: a complete structure solution, refinement and analysis program, *J. Appl. Crystallogr.* **2009**, *42*, 339–341.
7. M. Solar and N. Trapp, µCHILL: a lightweight, modular system for handling crystalline samples at low temperatures under inert conditions, *J. Appl. Crystallogr.* **2018**, *51*, 541–548.
8. A. L. Spek, *PLATON* SQUEEZE: a tool for the calculation of the disordered solvent contribution to the calculated strucutre factors, *Acta Crystallogr.* **2015**, *C71*, 9–18.